

N two-level atoms in a driven optical cavity: Quantum dynamics of forward photon scattering for weak incident fields

R. J. Brecha,¹ P. R. Rice,² and M. Xiao³

¹*Department of Physics, University of Dayton, Dayton, Ohio 45469*

²*Department of Physics, Miami University, Oxford, Ohio 45056*

³*Department of Physics, University of Arkansas, Fayetteville, Arkansas 72701*

(Received 16 September 1998)

We investigate the photon statistics of the light transmitted from a driven optical cavity containing N two-level atoms, with emphasis on the weak driving field limit. This limit is of most interest from the point of view of quantum fluctuations. We find that various types of nonclassical behavior are possible, even with large numbers of atoms in the cavity, under conditions of strong atom-field coupling, which we refer to as the cavity quantum electrodynamics limit. We describe the system with a pure-state formalism valid for weak fields, and also use a Fokker-Planck equation obtained by a small fluctuation linearization. We examine the conditions under which the linearized theory is appropriate, and explore the sensitivity of nonclassical effects in the system to atom number, transit-time broadening, and detunings. [S1050-2947(99)04803-9]

PACS number(s): 42.50.Ct, 42.50.Lc, 42.50.Ar

I. INTRODUCTION

In this paper we report on extensions of previous work on dynamical cavity quantum electrodynamics (cavity QED) effects, namely, the photon statistics of an ensemble of two-level atoms inside a driven optical cavity. The field of cavity QED can be said to have been born more than 40 years ago with the prediction by Purcell [1] that the spontaneous emission rate for an atom inside a conducting cavity can be greatly enhanced in comparison with the rate in free space if the dimensions of the cavity are of the order of the transition wavelength. The subject was only of theoretical interest until experimental techniques became available to observe such effects. In the first such measurement, Drexhage [2] observed the enhanced and inhibited decay rates of dye molecules located close to a dielectric surface. This effect can be interpreted as the reaction of the molecule to the image charges that effectively replace the reflecting surface [3]. The first experiments with atoms in a cavity were those of Vaidnathan, Spencer, and Kleppner [4], Goy *et al.* [5], and Jhe *et al.* [6]. Several later experiments have been carried out to investigate various features of the change in spontaneous emission rates due to the presence of boundaries which alter the electromagnetic field mode density from its free space value [7,8]. Accompanying the experimental work is a large body of theoretical literature concerning the same subject [9–12]. For a more detailed history of the field, as well as current developments, we refer the reader to the reviews of Hinds [13] and Haroche [14], and the compilation edited by Berman [15].

Another approach to what is now known as cavity QED had its beginnings in the work of Jaynes and Cummings [16] on the interaction of a single two-level atom with one mode of the electromagnetic field, and extensions of that work by Tavis and Cummings to consider many atoms [17,18]. This too was originally viewed as a purely theoretical construct, with no immediate realization in the laboratory possible, particularly as dissipation is not included in the model. How-

ever, with suitable modifications to allow for atomic and cavity field damping, there has been a great deal of work done, both theoretical and experimental, to gain a deeper understanding of this fundamental, and very rich, quantum system. Experiments to observe the dynamics of this system include maser action from a collection of several atoms or even one atom interacting with a single field mode in a resonator [19–23]. Nonclassical properties of the steady state in the cavity have also been investigated [23]. In the optical domain as well as at microwave frequencies there have been experiments to look at the so-called “vacuum-Rabi” splitting [24–30].

Yet another class of theory and experiments relevant to our discussion is the body of literature on resonance fluorescence, where a two-level atom interacts with a classical driving field. The three peaked Mollow spectrum and nonclassical effects such as photon antibunching and sub-Poissonian photon counting statistics have been predicted [31,32] and observed [33,34]. A review is given by Cresser *et al.* [35]. Squeezing has also been predicted [36], but not yet observed.

The model we consider here assumes N two-level atoms interacting with one mode of a resonator of arbitrary Q , with a driving field present, and we take into account both atomic and cavity field losses. This model can be thought of as resonance fluorescence in a cavity, the Tavis-Cummings model with a driving field and losses added, or an extension of previous work on optical bistability. We wish to stress that damping is not to be considered as an unfortunate consequence of modeling a real system, but rather as a fundamental property of the system we consider. The presence of a driving field and dissipation results in a nontrivial steady state for the system. Of course the ultimate importance of this work is the possibility of testing the theoretical results obtained herein in the laboratory, with a real dynamical system. We also stress that we will be interested in effects that can only be explained by quantization of the electromagnetic field, i.e., nonclassical effects.

In cavity quantum electrodynamics, one is concerned with

situations in which the atom-field coupling strength (g) is comparable to at least one of the dissipation rates set by spontaneous emission to noncavity modes (γ) and by cavity losses (κ); typically this requires that the cavity mode volume be small, or that the cavity enclose a large portion of $4\pi sr$ about the atom. We will be most concerned here with the strong-coupling limit, where g is the largest rate in the problem. In this strong-coupling regime, the atom cannot be thought of as mildly perturbed by the cavity field (bad-cavity limit) or the field as perturbed by the presence of the atom (good-cavity limit). Energy is exchanged between these two oscillators several times before dissipation has a significant effect.

There is a natural separation into two classes of phenomena. In the first set of phenomena the emphasis is on what we prefer to call “structural” properties of the atom-cavity interaction. Under this category we would put experiments in which alterations are observed in atomic fluorescence linewidths, a splitting of the atomic line (vacuum-Rabi splitting), or in which the interaction results in a shift of the system resonance frequency. These results can be obtained by considering the atom and cavity mode as coupled oscillators; indeed for weak driving fields the atom is approximated well by a harmonic oscillator. The second type of experiment involves investigation of the dynamical character of the atom-field system, and requires a fully quantum mechanical treatment of the field. Examples would include squeezing and photon antibunching. These phenomena cannot be explained by a simple coupled-oscillator theory. There have been several review articles in which one or both of these regimes of cavity QED have been discussed [13–15], as stated earlier.

It is this second class of systems that we wish to address in this paper. The structural effects in cavity QED can be seen to follow from several (essentially semiclassical) points of view. For weak fields, the atom and cavity can be viewed as two coupled harmonic oscillators [41], or alternatively the atoms can be treated as a dielectric medium with an index of refraction [27], giving rise to a vacuum-Rabi splitting. Alternatively, one can understand modification of spontaneous emission due to a mirror [12] in terms of an image charge radiating in or out of phase with the atom. Yet another way to view enhanced and suppressed spontaneous emission uses a Fermi’s golden rule argument, realizing that the mode density into which an atom may emit radiation is modified by the cavity boundary conditions. This argument is only really appropriate in the limit where the cavity decay rate is large compared to the atomic spontaneous emission rate, the so-called bad-cavity limit. In this limit the effect of the cavity on the atom may be treated as a perturbation, and spontaneous emission into the cavity mode is effectively an irreversible process due to the low Q of the cavity. In the strong-coupling regime, where the atom and cavity exchange a photon several times before it is lost, a picture based on perturbation theory is not appropriate.

Usually [38,39], one solves for the semiclassical steady state of the system, i.e., that which is obtained from the Heisenberg equations of motion when expectation values of products are factorized, and then examines the effects of small (quantum) perturbations on these steady states. In these theories, the small noise assumption is made, and hence, one may disallow oneself of the possibility of examining the sys-

tem in a regime where the effects of quantum noise are substantial. In many cases, as for the laser and optical bistability, the system size parameter that is used in the linearization is the saturation photon number, $\sqrt{n_s} = \gamma/2\sqrt{2}g$. The signal to noise ratio is on the order of n_s . A linearization based on the number of atoms may still work, but this approach will not necessarily work for a small number of atoms. In this regime, the coupling strength is assumed *a priori* to be smaller than the atomic spontaneous emission rate. Vacuum Rabi splittings may still be observed if $\sqrt{N}g$ is much larger than κ , the cavity energy loss rate, or if $\kappa \approx \gamma$ [40,41,26]. Hence vacuum Rabi splitting is **not** necessarily a manifestation of the quantum nature of the field, although it can certainly be understood in that manner. We are interested in the cavity QED regime, which we define by $(\bar{\gamma} - \gamma)/\gamma \approx 1$, where $\bar{\gamma}$ is the cavity enhanced spontaneous emission rate. This typically requires that $g \gg \gamma$, and hence the usual linearized theories, which assume n_s is large, may not necessarily work.

In previous work in this regime, for a single atom in the bad-cavity limit, and for weak driving fields, Rice and Carmichael [42] have found sub-Poissonian photon counting statistics, squeezing, photon antibunching, and the vanishing of $g^{(2)}(\tau)$ for nonzero delay time τ . This work was later extended to the many-atom case by Carmichael, Brecha, and Rice [43]. There it was emphasized that the effect persisted for N atoms, but only if the cavity QED condition was met. In many systems, the quantum noise scales as $1/N$, as, for example, photon antibunching in N -atom resonance fluorescence. We emphasize that as long as the “cavity QED condition” is met, the photon statistics are only weakly dependent on the number of atoms; qualitatively the behavior is the same as the single-atom case. Recently, photon antibunching has been observed in this system [44]. Mielke, Foster, and Orozco [45] have seen a further type of nonclassical behavior in this system, as predicted in Refs. [42,43]. In light of these experiments, it is important to consider this fundamental system in more detail.

In this paper we examine the formal rationale for the pure-state formalism used in Ref. [43]. The pure-state ansatz is used to obtain the steady-state density operator, which is then propagated using the standard methods of the quantum regression theorem. Connections to recent advances in modeling open systems, specifically quantum trajectory theory will be made. Further, we include the effects of detunings and transit-time broadening, and compare with the predictions of a more standard stochastic dynamical model, of the sort discussed above.

The very general outline of this paper is to look at the statistics of forward photon scattering, i.e., the light transmitted from the cavity, from two different points of views. First we will discuss the photon statistics resulting from the quantum dynamics of an *observed* pure state, and second, in the context of the formalism of a stochastic process in the positive- P representation [38,39]. In Sec. II we discuss the details of the physical system considered. The formal derivation leading to the use of pure-state dynamics even in the presence of dissipation is discussed in Sec. III. We turn to the photon statistics of the transmitted field in Sec. IV. In Sec. V, we make a comparison to coupled oscillator theory. Section VI discusses a stochastic dynamical model, which depends on a linearization using the number of atoms as a

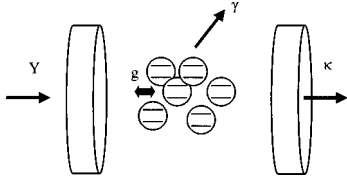


FIG. 1. Schematic of the physical system, N is the number of atoms in the cavity, κ is the cavity field damping rate, γ is the spontaneous emission rate to noncavity modes, and g is the atom-field coupling.

system size parameter. In Sec. VII, we use the stochastic model to calculate the photon statistics, and compare the results to those of Sec. IV. In Sec. VIII, we discuss the dependence of the photon statistics on a variety of parameters: atomic and cavity detunings Δ and Θ , number of atoms N , coupling parameter g , cavity loss rate κ , and atomic spontaneous emission rate γ . We use the stochastic model to discuss the effects of transit time broadening and/or phase destroying collisions on the photon statistics, an effect that cannot be treated using the pure-state formalism of Secs. III and IV. Finally, we conclude in Sec. IX.

II. PHYSICAL MODEL

The model to be treated is a generalization of the Jaynes-Cummings atom-field interaction, including the effects of both cavity and atomic decay as well as that of an external driving field. The system is shown schematically in Fig. 1. In one context, this is simply the microscopic model for optical bistability with two-level atoms in a cavity. The field and atomic Hamiltonians are given by

$$\hat{H}_F = \hbar \omega_c \hat{a}^\dagger \hat{a}, \quad (1a)$$

$$\hat{H}_A = \hbar \omega_a \hat{J}_z, \quad (1b)$$

respectively. In the rotating wave approximation the interaction Hamiltonian is given by

$$\hat{H}_{AF} = i\hbar g (\hat{a}^\dagger \hat{J}_- - \hat{a} \hat{J}_+). \quad (2)$$

In the above, ω_c (ω_a) is the resonance frequency of the cavity (atomic transition). The cavity field creation and annihilation operators are given by \hat{a}^\dagger and \hat{a} , respectively. $g = \mu_0(\omega_c/2\hbar\epsilon_0 V_Q)^{1/2}$, where μ_0 is the dipole transition matrix element, and V_Q is the cavity mode volume. The collective atomic operators are given by

$$\hat{J}_\pm = \sum_{j=1}^N e^{\pm ikz_j} \sigma_\pm^j, \quad (3a)$$

$$\hat{J}_z = \sum_{j=1}^N \sigma_z^j, \quad (3b)$$

where σ_\pm and σ_z are the Pauli spin operators describing the two-level atomic system. Following standard techniques the atomic population and polarization decay, as well as the field damping can be described by the action of the Liouville operators on the density matrix of the system [38,39]:

$$L_{irrev}^A \rho = \frac{\gamma_{\parallel}}{2} \sum_{j=1}^N (2\sigma_-^j \rho \sigma_+^j - \sigma_+^j \sigma_-^j \rho - \rho \sigma_+^j \sigma_-^j) + (\gamma_{\parallel} - 2\gamma_{\perp}) \sum_{j=1}^N (\sigma_z^j \rho \sigma_z^j - \rho), \quad (4a)$$

$$L_{irrev}^F \rho = \kappa (2\hat{a} \rho \hat{a}^\dagger - \hat{a}^\dagger \hat{a} \rho - \rho \hat{a}^\dagger \hat{a}). \quad (4b)$$

For the experiments designed to observe the effects to be described throughout this paper, visible or near visible wavelength atomic transitions are well suited, in which case thermal photon numbers are completely negligible and thus these terms have been omitted in the damping term. It would be a straightforward generalization to include the effects of thermal photons, and this would indeed be necessary for a description of systems involving Rydberg atoms coupled to microwave cavities.

For completeness, we consider here a general formulation of the damping in which nonradiative decay processes are possible, i.e., $\gamma_{\parallel} \neq 2\gamma_{\perp}$. Much of what we will discuss in this paper assumes purely radiative atomic decay ($\gamma_{\parallel} = 2\gamma_{\perp}$); for example, the pure state formalism introduced in Sec. III will only be valid in this limit. In Secs. VI and VIII we will address departures from the purely radiative regime. Since one goal of the present work is to realistically describe an experimental situation, it should be noted here that the departure from purely radiative decay in present experiments [44,45] is small and only quantitative differences are to be expected.

The final term to be considered is that describing the driving field-cavity field interaction, which is given by

$$\hat{H}_{LF} = i\hbar (E e^{-i\omega_0 t} \hat{a}^\dagger - E^* e^{i\omega_0 t} \hat{a}), \quad (5)$$

where E is the scaled (classical) input laser field strength. The scaling is such that E/κ is the photon flux injected into the cavity by the driving field. We note that treating this driving field quantum mechanically, and assuming it is a highly excited coherent state produces the same results.

The master equation for the full system is now given by

$$\dot{\rho} = (-i/\hbar) [\hat{H}_A + \hat{H}_F + \hat{H}_{AF} + \hat{H}_{LF}, \rho] + L_{irrev}^A \rho + L_{irrev}^F \rho \equiv \mathcal{L}\rho, \quad (6)$$

which will be the starting point for the rest of the paper.

III. PURE-STATE DYNAMICS FOR WEAK FIELDS AND RADIATIVE DAMPING

Here, we begin with equations of motion for density matrix elements. As we are going to consider the limit $E \rightarrow 0$, we truncate our basis set at some level. As we wish to calculate the second-order intensity correlation function $g^{(2)}(\tau)$, we must keep states with two quanta of energy at a minimum. We will then use the truncated basis

$$|00\rangle, |10\rangle, |01\rangle, |20\rangle, |11\rangle, |02\rangle. \quad (7)$$

Here, the first index corresponds to the number of energy quanta in the atoms, and the second corresponds to the excitation of the field. This is an incomplete specification of the

state of the system, as, for example, in the state $|10\rangle$, the quantum of energy could be stored in any one of the N atoms. In actuality then, we have $(1)+(N)+(1)+(N[N-1])+(N)+(1)=N^2+N+3$ states here. The numbers in the previous sum represent the number of real states of the system that correspond to the generic states (7). We assume that all atoms couple to the field with the same Jaynes-Cummings parameter g , i.e., that they are all at antinodes of the field, for example, and that all of the atoms are identical. Under these conditions one may use a symmetrized set of atomic states that reflects the permutation symmetry required for identical atoms, as we show in Appendix A. A relaxation of this assumption that allows for numerical computation is described in [44]. So instead of considering a set of atomic states such as

$$\begin{aligned} |1\rangle &= |\downarrow_1 \downarrow_2 \dots \downarrow_{k-1} \uparrow_k \downarrow_{k+1} \dots \downarrow_N\rangle, \\ |2\rangle &= |\downarrow_1 \downarrow_2 \dots \downarrow_{k-1} \uparrow_k \downarrow_{k+1} \dots \downarrow_{l-1} \uparrow_l \downarrow_{l+1} \dots \downarrow_N\rangle, \\ & \quad l \neq k, \end{aligned} \quad (8)$$

we define the symmetric states

$$\begin{aligned} |1\rangle_s &= \frac{1}{\sqrt{N}} \sum_{k=1}^N |\downarrow_1 \downarrow_2 \dots \downarrow_{k-1} \uparrow_k \downarrow_{k+1} \dots \downarrow_N\rangle, \\ |2\rangle_s &= \frac{2}{\sqrt{N(N-1)}} \sum_{k=1}^N \sum_{\substack{l=1 \\ l \neq k}}^N \\ & \quad \times |\downarrow_1 \downarrow_2 \dots \downarrow_{k-1} \uparrow_k \downarrow_{k+1} \dots \downarrow_{l-1} \uparrow_l \downarrow_{l+1} \dots \downarrow_N\rangle, \\ & \quad l \neq k. \end{aligned} \quad (9)$$

These are then the atomic states referred to in Eq. (7). In this truncated basis we then have 21 independent density matrix elements. Initially, we restrict our calculation to zero atomic and cavity detuning, and hence these density matrix elements are all real. In Sec. VIII, we shall return to the effect of these detunings on our results. We also consider the limit of purely radiative broadening here, and address the ramifications of the relaxation of that assumption in Sec. VIII. The set of equations that must be solved are then given in Appendix A.

Here we define $C = Ng^2/\kappa\gamma$ and $\mu = 2\kappa/\gamma$, and time is scaled by $\gamma/2$. The density matrix elements are scaled according to the relation

$$\rho_{n,l;m,k} \rightarrow n_s^{(n+m)/2} Y^{(n+m+l+k)} \rho_{n,l;m,k}, \quad (10)$$

where Y is a dimensionless driving field and $n_s = \gamma_{\parallel} \gamma_{\perp} / 4g^2 = 1/4\mu C_1$ is the saturation photon number.

At this point, we examine the possibility of using a pure-state description for the dynamics of this system. In the one-atom case, in the bad-cavity limit, we have previously solved for the steady-state density matrix elements, and find that they are consistent with a pure-state factorization of the density matrix. Outside the bad-cavity limit, numerical results indicate that this is still the case. Here, we wish to see if the density matrix for this system can be represented by

$$\rho = |\psi(t)\rangle\langle\psi(t)|. \quad (11)$$

As we have truncated our basis at the two-photon level, we postulate that the state of the system is of the form

$$\begin{aligned} |\psi(t)\rangle &= |00\rangle + Y D_{01}(t) |01\rangle + \sqrt{n_s} Y D_{10}(t) |10\rangle \\ & \quad + Y^2 D_{02}(t) |02\rangle + \sqrt{n_s} Y^2 D_{11}(t) |11\rangle \\ & \quad + n_s Y^2 D_{20}(t) |20\rangle. \end{aligned} \quad (12)$$

This wave function is normalized to lowest order in Y . If such a factorization of the density matrix is possible, the density matrix elements must be related to the complex probability amplitudes above via equations of the form

$$\rho_{ij;ij} = |D_{ij}|^2, \quad (13a)$$

$$\rho_{ij;kl} = D_{ij}^* D_{kl}. \quad (13b)$$

As $D_{00} = 1$ (to order Y) in the weak-field limit, that means that we must have

$$\rho_{00;ij} = D_{ij}. \quad (14)$$

Thus we may use the equations for the matrix elements $\rho_{00;ij}$ to write down a proposed set of equations for the probability amplitudes as

$$\dot{D}_{01} = \frac{-\sqrt{N}}{2\sqrt{2}} D_{10} - \frac{1}{2} D_{01}, \quad (15a)$$

$$\dot{D}_{02} = \frac{-\sqrt{N-1}}{\sqrt{2}} D_{11} - D_{02}, \quad (15b)$$

$$\dot{D}_{10} = \sqrt{2N}\mu C D_{01} - \frac{\mu}{2} D_{10} + \frac{\mu}{2}, \quad (15c)$$

$$\begin{aligned} \dot{D}_{11} &= \frac{-\sqrt{N}}{2} D_{20} + \sqrt{2}\mu C \left(1 - \frac{1}{N}\right) D_{02} + \frac{\mu}{2} D_{01} \\ & \quad - \frac{1}{2} (1 + \mu) D_{11}, \end{aligned} \quad (15d)$$

$$\dot{D}_{20} = 2\mu C D_{11} + \frac{\mu}{2\sqrt{2}} D_{10} - \mu D_{20}. \quad (15e)$$

The dot refers to differentiation with respect to the scaled time γt .

We must now check that the other density matrix element equations are of a form that is consistent with a pure state factorization. We consider an example below:

$$\begin{aligned} \dot{\rho}_{01;01} &= 2D_{01}\dot{D}_{01} = -\frac{1}{\sqrt{2}} D_{01} D_{10} - D_{01} D_{01} \\ & = -\frac{1}{\sqrt{2}} \rho_{01;10} - \rho_{01;01}, \end{aligned} \quad (16)$$

which shows that in this case the equations are of the form one would obtain by using a pure state given as above. Upon checking the other 15 equations, we find indeed that the density matrix element equations are consistent with the system

as described by the pure state [Eq. (12)]. It is not immediately obvious why a system with dissipation obeys pure-state dynamics. We stress that this is not an approximation introduced *ad hoc*, but that in the weak-field limit, for radiative damping, the dynamics of the system can be described by the pure-state evolution given by Eqs. (15). In quantum mechanics, a system evolves in two ways: (i) by unitary evolution via the propagator, determined by the Hamiltonian, and (ii) random collapses due to dissipation. The probability of a collapse is proportional to the rate of dissipation (κ or γ) as well as the probability for the system to have energy in it (i.e., the number of intracavity photons or number of atoms in the excited state). As the excitation probability is small in the weak-field limit, so is the probability of a collapse. Hence in this weak-field limit, the system can be described by a pure state even in the presence of dissipation, at least during the time between two-photon emissions. Thus this approach is appropriate for a calculation of $g^{(2)}(\tau)$, providing that we start with the state of the system *given* that it has emitted a photon, and calculate the probability of a subsequent emission at time τ . In one sense the calculation of $g^{(2)}(\tau)$ presented here is really a calculation of the waiting time distribution, i.e., $W(\tau)$, the probability that the *next* photon arrives at τ , with none arriving in between. For weak fields, the probability of another photon arriving in the interval $0 \rightarrow \tau$ is vanishingly small, and the difference between $W(\tau)$ and $g^{(2)}(\tau)$ vanishes. In most experiments [34] the waiting time distribution is the quantity actually measured, and for weak fields, this corresponds to a measurement of $g^{(2)}(\tau)$ [46].

More properly, as we deal with an open system that cannot be described by a wave function, we can think in terms of the quantum trajectory theory developed by Carmichael [47], Dalibard, Caston, and Molmer [48], and Dum, Zoller, and Ritsch [49]. Here we follow the approach of Carmichael, which consists of an unravelling of the master equation into evolution and collapse processes, with the collapse occurring randomly. Dissipative systems are described by wave functions that evolve via a nonunitary Hamiltonian or a collapse operator. Numerically, a random number generator weighted by the probability of a collapse determines which process takes place at a given time step. As both processes are non-unitary, the wave function is then renormalized, and one throws another random number. One then averages over an ensemble of these conditioned wave functions to obtain statistical information. Here again, the probability of a collapse is related to dissipation rates as well as excitation probability. It is the latter that is small in the weak-field limit, and hence the time between collapses is relatively long. As $D_{00} \approx 1$ and the other probability amplitudes are proportional to some power of Y , for weak fields the wave function (12) is normalized to leading order in Y , and the evolution preserves the norm to that same order. Our results will then be valid only in the limit that $Y \rightarrow 0$. A sample trajectory obtained by the method of Carmichael is shown in Fig. 2.

In the bad-cavity limit, weak fields means approximately 10% of the saturation field; in the good-cavity limit, the field must be much smaller. Recent work by Alsing and Savage, and Rice and Clemens deal with how small the field must be for the system to be accurately approximated in this fashion for more than one atom [50,51].

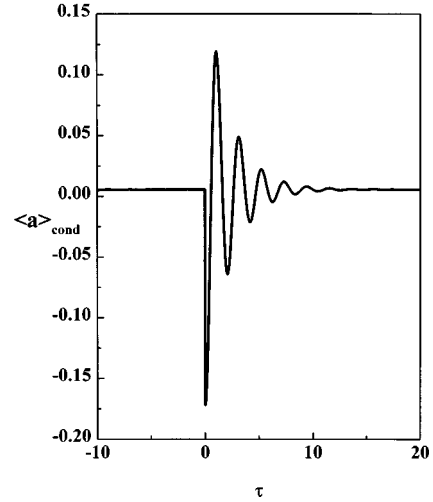


FIG. 2. Intracavity field conditioned on emission of photon at $\tau=0.0$ calculated using a quantum trajectory algorithm. The curve is for $g/\gamma=3.0$, $\kappa/\gamma=0.5$, and $Y/\gamma=0.1$.

IV. PHOTON STATISTICS OF THE TRANSMITTED FIELD

A. Coincident photon count rates

At times long compared to γ^{-1} and κ^{-1} , the asymptotic steady state reached by the system is

$$|\psi_{SS}\rangle = |00\rangle + YD_{01}^{SS}|01\rangle + \sqrt{n_s}YD_{10}^{SS}|10\rangle + Y^2D_{02}^{SS}|02\rangle + \sqrt{n_s}Y^2D_{11}^{SS}|11\rangle + n_sY^2D_{20}^{SS}|20\rangle, \quad (17)$$

where

$$D_{01}^{SS} = \frac{-1}{\sqrt{2}} \frac{1}{1+2C}, \quad (18a)$$

$$D_{10}^{SS} = \frac{1}{1+2C}, \quad (18b)$$

$$D_{02}^{SS} = \frac{1}{2(1+2C)} \frac{1}{1+2C-2C_1(\mu/(1+\mu))}, \quad (18c)$$

$$D_{11}^{SS} = \frac{1}{\sqrt{2}(1+2C)} \frac{1}{1+2C-2C_1(\mu/(1+\mu))}, \quad (18d)$$

$$D_{20}^{SS} = \frac{1}{2(1+2C)} \left[1 - \frac{2C}{1+2C-2C_1(\mu/(1+\mu))} \right], \quad (18e)$$

where we have defined $C_1 = C/N = g^2/\kappa\gamma$.

We may calculate the steady-state average intracavity field and photon number, to lowest order in Y ,

$$\langle \hat{a} \rangle_{SS} = \langle \psi_{SS} | \hat{a} | \psi_{SS} \rangle \approx C_{10} = \sqrt{n_s} \frac{Y}{1+2C}, \quad (19)$$

$$\langle \hat{a}^\dagger \hat{a} \rangle_{SS} = \langle \psi_{SS} | \hat{a}^\dagger \hat{a} | \psi_{SS} \rangle \approx |C_{10}|^2 = \frac{n_s Y^2}{(1+2C)^2}. \quad (20)$$

We may also construct the steady-state value of $g^{(2)}(0)$, resulting in

$$g^{(2)}(0) = \frac{\langle \psi_{SS} | \hat{a}^{\dagger 2} \hat{a}^2 | \psi_{SS} \rangle}{\langle \psi_{SS} | \hat{a}^{\dagger} \hat{a} | \psi_{SS} \rangle^2} \approx \frac{2|C_{20}|^2}{|C_{10}|^4} = \left[1 - 4CC_1 \frac{\mu}{1+\mu} \frac{1}{1+2C-2C'_1} \right]^2, \quad (21)$$

where $C'_1 = C_1(1+1/\mu)^{-1}$. For $N \gg 1$, this reduces to

$$g^{(2)}(0) = \left[1 - \frac{1}{N} \frac{4C^2}{1+2C} \frac{\mu}{1+\mu} \right]^2. \quad (22)$$

This agrees with the result given by a linearized treatment of quantum fluctuations, if higher-order fluctuations are kept, as discussed in Sec. VII, where the number of atoms N is used as a system size parameter [52]. It will sometimes be convenient to consider $g^{(2)}(0)$ in the following form:

$$g^{(2)}(0) = \left[\frac{(1+2C)(1-2C'_1)}{1+2C-2C'_1} \right]^2. \quad (23)$$

We postpone a discussion of this result until later in the paper.

B. Delayed Coincidence rates from pure-state dynamics

In formal language, using the quantum regression theorem, the joint photodetection probability is given by [39]

$$(2\eta\kappa T)^2 \langle a^\dagger(0)a^\dagger(\tau)a(\tau)a(0) \rangle = (2\eta\kappa T)^2 \text{tr}[a^\dagger a e^{\mathcal{L}\tau}(a\rho_{SS}a^\dagger)], \quad (24)$$

where \mathcal{L} is the Liouvillian operator in the master equation $\dot{\rho} = \mathcal{L}\rho$. This may be written as the product of two probabilities:

$$(2\eta\kappa T)^2 \langle a^\dagger(0)a^\dagger(\tau)a(\tau)a(0) \rangle = [2\eta\kappa T \text{tr}(\bar{\rho}(\tau)a^\dagger a)] [2\eta\kappa T \langle a^\dagger a \rangle_{SS}], \quad (25)$$

where

$$\bar{\rho}(\tau) = e^{\mathcal{L}\tau}(a\rho_{SS}a^\dagger / \langle a^\dagger a \rangle_{SS}) \quad (26)$$

is the density operator that evolves via the master equation from the initial state,

$$\bar{\rho}(0) = a\rho_{SS}a^\dagger / \langle a^\dagger a \rangle_{SS}. \quad (27)$$

The two probabilities on the right-hand side of Eq. (25) have simple interpretations: $2\eta\kappa T \langle a^\dagger a \rangle$ is the probability for detecting a first photon at $\tau=0$; $(2\eta\kappa T) \text{tr}(\bar{\rho}(\tau)a^\dagger a)$ is the probability for detecting a second photon at a time τ with the system in the state $\bar{\rho}(\tau)$, which has evolved from the reduced state $\bar{\rho}(0)$ prepared by the first photodetection, describing the instantaneous state of the system after the detection of the first photon.

The density matrix $\bar{\rho}(0)$ can be written as

$$\bar{\rho}(0) = |\psi_{col}\rangle \langle \psi_{col}|. \quad (28)$$

At this point we ask, when the system is in steady state, and a photon is detected in the transmitted field, what is the reduced state? We find from Eq. (27), with $\rho_{SS} = |\psi_{SS}\rangle \langle \psi_{SS}|$,

$$|\psi_{col}\rangle = \frac{\hat{a}|\psi_{SS}\rangle}{\sqrt{\langle \psi_{SS} | \hat{a}^\dagger \hat{a} | \psi_{SS} \rangle}}. \quad (29)$$

This may be written in the form

$$|\psi_{col}\rangle = |00\rangle + D_{01}^{col}|01\rangle + D_{10}^{col}|10\rangle, \quad (30)$$

where

$$D_{01}^{col} = \frac{D_{11}^{SS}}{D_{10}^{SS}}, \quad (31a)$$

$$D_{10}^{col} = \frac{\sqrt{2}D_{20}^{SS}}{D_{10}^{SS}}. \quad (31b)$$

We now calculate the state of the system at time τ given that it was in the state ψ_{col} at $\tau=0$. This is given by the solution to the probability amplitude Eqs. (15) with initial conditions given by Eq. (31). We then have for the second-order intensity correlation function,

$$g^{(2)}(\tau) = \frac{|D_{10}^{col}(\tau)|^2}{|D_{10}^{SS}|^2}. \quad (32)$$

Here D_{10}^{col} is the probability amplitude for all atoms to be in the ground state and one photon in the cavity, at time $\tau=0$, given that the system was in the collapsed state $|\psi_{col}\rangle$ at time 0. Obviously, we need only keep one photon states in this reduced state in order to calculate $g^{(2)}(\tau)$, which involves the detection of the second photon.

The final result of this calculation for $g^{(2)}(\tau)$ is [43]

$$g^{(2)}(\tau) = \left\{ 1 + \frac{\Delta\alpha}{\alpha} \exp\left[-\frac{1}{4}(\mu+1)\tau\right] \times \left[\cosh \Omega\tau + \frac{(\mu+1)}{4\Omega} \sinh \Omega\tau \right] \right\}^2, \quad (33)$$

where

$$\frac{\Delta\alpha}{\alpha} = -2C'_1[2C/(1+2C-2C'_1)] \quad (34)$$

and

$$\Omega = (1/4)\sqrt{(\mu-1)^2 - 4Ng^2}, \quad (35)$$

and we have $C_1 = g^2/\kappa\gamma$ and $C'_1 = C_1/(1+\gamma/2\kappa) = C_1/(1+1/\mu)$.

This expression depends on the number of atoms only through the difference between C and C'_1 , and in the value of the Rabi frequency Ω . For a large number of atoms and large coupling, the factor $\Delta\alpha/\alpha$ reduces to

$$\frac{\Delta\alpha}{\alpha} = -2C'_1, \quad (36)$$

a quantity that is independent of the number of atoms. The size of $g^{(2)}(0)$ is independent of the number of atoms (for $N \gg 1$), and relaxation to the steady state occurs at a rate determined by the collective coupling constant $\sqrt{N}g$. For $N = 1$ and in the bad-cavity limit ($\mu \rightarrow \infty$), this result reduces to that of Ref. [42].

It is a straightforward task to include the effect of detunings on $g^{(2)}(\tau)$. The master equation is modified in the following manner:

$$\kappa \rightarrow \kappa(1 + i\Theta) \equiv \tilde{\kappa}, \quad (37)$$

$$\gamma \rightarrow \gamma(1 + 2i\Delta) \equiv \tilde{\gamma}, \quad (38)$$

where $\Delta = 2(\omega_a - \omega_0)/\gamma$ and $\Theta = (\omega_c - \omega_0)/\kappa$ are dimensionless atomic and cavity detunings, respectively. Formally then, the matrix element equations, and hence the equation for the pure state probability amplitudes are modified in the exact same manner, with the result

$$\dot{D}_{01} = \frac{-1}{2\sqrt{2}}D_{10} - \left(\frac{1}{2} + i\Delta\right)D_{01}, \quad (39a)$$

$$\dot{D}_{02} = \frac{-1}{\sqrt{2}}D_{11} - (1 + 2i\Delta)D_{02}, \quad (39b)$$

$$\dot{D}_{10} = \sqrt{2}\mu CD_{01} \left(\frac{\mu}{2} + i\Theta\right)D_{10} + \frac{\mu}{2}, \quad (39c)$$

$$\begin{aligned} \dot{D}_{11} = & \frac{-1}{2}[1 + \mu + 2i(\Delta + \Theta)]D_{20} + \sqrt{2}\mu C \left(1 - \frac{1}{N}\right)D_{02} \\ & + \frac{\mu}{2}D_{01} - \frac{1}{2}D_{11}, \end{aligned} \quad (39d)$$

$$\dot{D}_{20} = 2\mu CD_{11} + \frac{\mu}{2\sqrt{2}}D_{10} - (\mu + 2i\Theta)D_{20}. \quad (39e)$$

The density matrix equations are still equivalent to those obtained from the above equations for probability amplitudes. The dot in the above equations still signifies differentiation with respect to γt , not with respect to the above-defined complex $\tilde{\gamma}$. The resulting expression for $g^{(2)}(\tau)$ is then

$$\begin{aligned} g^{(2)}(\tau) = & \left| 1 + \frac{\Delta\tilde{\alpha}}{\tilde{\alpha}} \exp\left[-\frac{1}{2}(\tilde{\kappa} + \tilde{\gamma}/2)\tau\right] \right. \\ & \left. \times \left[\cosh \tilde{\Omega}\tau + \frac{(\tilde{\kappa} + \tilde{\gamma}/2)}{2\tilde{\Omega}} \sinh \tilde{\Omega}\tau \right] \right|^2, \end{aligned} \quad (40)$$

where

$$\frac{\Delta\tilde{\alpha}}{\tilde{\alpha}} = -2\tilde{C}'_1[2\tilde{C}/(1 + 2\tilde{C} - 2\tilde{C}'_1)] \quad (41)$$

with

$$\tilde{\Omega} = \sqrt{(1/4)(\tilde{\kappa} - \tilde{\gamma}/2)^2 - Ng^2} \quad (42)$$

and

$$\tilde{C} = Ng^2/\tilde{\kappa}\tilde{\gamma},$$

$$\tilde{C}'_1 = (g^2/\tilde{\kappa}\tilde{\gamma})(1 + 1/\tilde{\mu})^{-1},$$

$$\tilde{\mu} = 2\tilde{\kappa}/\tilde{\gamma}. \quad (43)$$

V. COMPARISON WITH COUPLED OSCILLATOR THEORY

Let us compare the results obtained in previous sections with those obtained by considering a pair of coherently driven coupled harmonic oscillators. Recall that structural cavity QED effects, such as linewidth enhancements and level shifts can be explained, at least qualitatively, using such a treatment. We take our lead from the equations for the probability amplitudes,

$$\dot{D}_{01} = \frac{-1}{2\sqrt{2}}D_{10} - \frac{1}{2}D_{01}, \quad (44)$$

$$\dot{D}_{10} = \sqrt{2}\mu CD_{01} - \frac{\mu}{2}D_{10} + \frac{\mu}{2}. \quad (45)$$

These equations formally describe coupled oscillators, with D_{01} and D_{10} the mean amplitudes of the atomic polarization and cavity field, respectively. As an example of how these equations contain structural cavity QED effects, let us consider the bad-cavity limit, defined by $\kappa \gg \gamma$, or $\mu \gg 1$. Then we may adiabatically eliminate D_{10} by setting $\dot{D}_{10} = 0$, to obtain

$$\dot{D}_{01} = -\frac{1}{2}(1 + 2C)D_{01} + \frac{1}{\sqrt{2}}. \quad (46)$$

Here we see that the atomic oscillator is damped at the cavity enhanced rate $(\gamma/2)(1 + 2C)$, where $C = Ng^2/\kappa\gamma$. It can also be shown that if the cavity is detuned, that the overall spontaneous emission rate can be reduced, to $(1 + 2C)/(1 + \Delta^2)$.

In Appendix B, we discuss how a pair of coherently driven coupled oscillators starting in a coherent state (for example, the ground state of the harmonic oscillator) evolves into a product state, where each oscillator is in a coherent state with a mean amplitude that comes from the two structural equations (45). Again, treating the atom as a simple harmonic oscillator is a good approximation in the weak-field limit, when the atom is predominantly in the ground state, i.e., $\langle \sigma_z \rangle \approx -1$. Formally this can be done using the Schwinger representation [37]. The amplitudes of the coherent states obey the following equations:

$$\dot{\alpha}_0 = -(\kappa_a + \omega_a)\alpha_0 + g\beta_0 + \mathcal{E}, \quad (47)$$

$$\dot{\beta}_0 = -(\kappa_b + \omega_b)\beta_0 + g\alpha_0. \quad (48)$$

A product of two coherent states can be expanded to find

$$\begin{aligned} |\alpha_0\rangle|\beta_0\rangle &= e^{-|\alpha_0|^2/2} [|0\rangle_a + \alpha_0|1\rangle_a + \alpha_0^2|2\rangle_a + \dots] \\ &\quad \times e^{-|\beta_0|^2/2} [|0\rangle_b + \beta_0|1\rangle_b + \beta_0^2|2\rangle_b + \dots] \\ &= \exp[-(|\alpha_0|^2 + |\beta_0|^2)/2] [|0\rangle_a|0\rangle_b + \alpha_0|1\rangle_a|0\rangle_b \\ &\quad + \beta_0|1\rangle_b|0\rangle_a + \alpha_0^2|2\rangle_a|0\rangle_b + \alpha_0\beta_0|1\rangle_a|1\rangle_b \\ &\quad + \beta_0^2|0\rangle_a|2\rangle_b + \dots]. \end{aligned} \quad (49)$$

Hence we see that, for the system to be described by a pair of oscillators, we must have the following condition on the probability amplitudes:

$$D_{02} = D_{01}^2 / \sqrt{2}, \quad (50a)$$

$$D_{11} = D_{10}D_{01}, \quad (50b)$$

$$D_{20} = D_{10}^2 / \sqrt{2}. \quad (50c)$$

This is consistent with the amplitude, Eqs. (15), if we make the replacement $\sqrt{N-1} \rightarrow \sqrt{N}$. It appears then that the coupled harmonic oscillator model explains the quantum fluctuations up to corrections of order $1/N$. However, this conclusion is too hasty. Consider the steady-state solution to the amplitude Eqs. (15):

$$\begin{aligned} |\psi\rangle &= |00\rangle + \alpha_0|10\rangle + \beta_0|01\rangle + (\alpha_0^2/\sqrt{2})pq|20\rangle \\ &\quad \times (\alpha_0\beta_0)q|11\rangle + (\beta_0^2/\sqrt{2})qr|20\rangle \end{aligned} \quad (51)$$

with

$$\begin{aligned} p &= 1 - 2C'_1, \\ q &= (1 + 2C)/(1 + 2C + 2C'_1), \\ r &= \sqrt{1 - 1/N}. \end{aligned} \quad (52)$$

The coupled oscillator model would have $r = p = q = 1$. In fact, q and r differ from unity by order of $1/N$, p differs from unity by $2C'_1 \approx (\bar{\gamma} - \gamma)/\gamma$, a quantity that is *independent of N* . This term is obviously only important when the cavity QED condition is met. Essentially, under cavity QED conditions, while the fluctuations are small, so is the mean intensity, and so quantum noise plays a very important role in system dynamics. The coupled oscillator theory would predict $g^{(2)}(\tau) = 1$ for all τ . Nonclassical behavior in the photon statistics arises only in the cavity QED regime, and hence we refer to this as a *dynamical cavity QED effect*; one that cannot be explained by coupled oscillator theory.

VI. A STOCHASTIC DYNAMICAL MODEL

The master equation of Sec. II will be used as the starting point for a more standard treatment of this problem, a formulation that in this case has its origins in the quantum theory of optical bistability [53] using a linearized Fokker-Planck for a positive- P distribution. The major purpose of pursuing this calculation is to examine how well the standard methods work in the regime of very few atoms and photons.

There is no *a priori* reason that the traditional methods, which require a system size expansion on the grounds that there are many atoms and/or photons should give results that are correct in the limit of one atom and/or photon, and we will examine the level of agreement between the two approaches. This will be a useful guide in discussing system size, for the purposes of using the linearized positive- P theory. The pure-state approach breaks down when one includes nonradiative broadening; these effects can be handled in the linearized positive- P approach, and will be considered.

We wish to derive a Fokker-Planck equation for a quasiprobability distribution function, and to be able to interpret it as such, and we desire that the diffusion of the probability be positive definite. The derivation of this Fokker-Planck equation and the difficulties with nonpositive definite diffusion have been discussed many times and therefore only an outline of the procedure will be given here. Since we are interested in the photon statistics of the light transmitted from the cavity, a natural selection for the quasiprobability distribution would be that of Glauber [54] and Sudarshan [55], the so-called P distribution, which allows one to describe averages of normally ordered field operators, corresponding to the detection (annihilation) of photons in a detector. The disadvantage to this approach at first sight is that the above-mentioned problem of non-positive-definite diffusion does indeed appear in the P representation. A generalization of the Glauber-Sudarshan P distribution is the positive P representation of Drummond and Gardiner [56] in which the system, nominally in five dimensions, is allowed to expand into ten dimensions. This is accomplished by making the field, polarization, and inversion variables into independent complex variables (i.e., $\alpha = \alpha_x + i\alpha_y$, $\alpha_* = \alpha_{*x} = i\alpha_{*y}$, where $\alpha_* \neq \alpha^*$). In the end, the quantities of interest are the averages of the stochastic variables, and in the mean, (α, α_*) , (v, v_*) are complex conjugate and m is real, but individual stochastic trajectories describing these variables are in fact allowed to explore the enlarged phase space.

First a characteristic function can be written as

$$\Xi(\beta, \beta_*, \xi, \xi_*, \eta) = \text{tr}(\rho e^{i(\beta_* \hat{a}^\dagger)} e^{i(\beta \hat{a})} e^{i(\xi J_+)} e^{i(\eta J_z)} e^{i(\xi J_-)}), \quad (53)$$

where $(\beta, \beta_*, \xi, \xi_*, \eta)$ are all independent complex variables. Usually the characteristic function can be defined as the Fourier transform of the desired quasiprobability distribution; in this case we define the relation as

$$\begin{aligned} \Xi(\beta, \beta_*, \xi, \xi_*, \eta) &= \int d^2\beta \int d^2\beta_* \int d^2\xi \int d^2\xi_* \int d^2\eta \\ &\quad \times P(\alpha, \alpha_*, v, v_*, m) e^{-i(\beta_* \alpha_*)} e^{-i(\beta \alpha)} e^{-i(\xi v)} \\ &\quad \times e^{-i(\eta m)} e^{-i(\xi v_*)}. \end{aligned} \quad (54)$$

Expectation values for operators can be expressed as derivatives of the characteristic function evaluated for zero argument, as in derivations in the P representation.

The results given here can be rigorously shown for the case of bosons [56]. Using standard techniques a Fokker-Planck equation for P can be derived that has the characteristic of being positive definite and therefore can be inter-

preted as a classical-type probability distribution, although in a ten-dimensional space. We will skip a detailed discussion of the Fokker-Planck equation and concentrate more on the associated Ito stochastic differential equations from which the linearized theory follows.

A set of Ito stochastic differential equations can be derived for this system that gives an equivalent description to that of the Fokker-Planck equation in the positive- P representation. These equations are more amenable to computer simulation, a topic which has been discussed in Ref. [57]. The set of equations, with atomic and cavity detunings, but allowing for nonradiative broadening is (from Ref. [57]):

$$d\alpha = (-\kappa(1+i\Delta)\alpha + g\nu + \varepsilon)dt, \quad (55a)$$

$$d\alpha_* = (-\kappa(1-i\Delta)\alpha_* + g\nu_* + \varepsilon)dt, \quad (55b)$$

$$d\nu = (-\gamma_{\perp}(1+i\Theta)\nu + 2g\alpha m)dt + [2g\alpha\nu]^{1/2}dW_1, \quad (55c)$$

$$d\nu_* = (-\gamma_{\perp}(1-i\Theta)\nu_* + 2g\alpha_* m)dt + [2g\alpha_*\nu_*]^{1/2}dW_2, \quad (55d)$$

$$dm = -\left[\gamma_{\parallel}\left[\frac{N}{2} + m\right] + g(\alpha\nu_* + \alpha_*\nu)\right]dt + \left[\gamma_{\parallel}\left[\frac{N}{2} + m\right] - g(\alpha\nu_* + \alpha_*\nu)\right]^{1/2}dW_3, \quad (55e)$$

where $\alpha = \alpha_x + i\alpha_y$ is the complex field variable in the Fokker-Planck equation referred to above and with α_* giving the intracavity intensity in units of photon number. As noted, in the positive- P representation, the variable α_* is not the complex conjugate of α but rather an independent complex variable.

The same holds for ν and ν_* , the polarization variables. Finally, m is the variable describing the atomic inversion and is complex as well. The variables dW_1 , dW_2 , and dW_3 are independent Wiener noise increments. In the absence of these noise terms one can solve for the steady-state solutions of the above equations directly:

$$\bar{\nu} = \bar{\alpha}m, \quad (56)$$

$$\bar{\nu}_* = \bar{\alpha}_*m, \quad (57)$$

$$\bar{m} = -\frac{1}{1 + \bar{\alpha}_*\bar{\alpha}}, \quad (58)$$

where the scaled variables are given by

$$\bar{\alpha} = n_s^{-(1/2)}\alpha, \quad (59a)$$

$$\bar{\alpha}_* = n_s^{-(1/2)}\alpha_*, \quad (59b)$$

$$\bar{\nu} = \left(\frac{N}{2}\right)^{-1} \left(\frac{\gamma_{\perp}}{\gamma_{\parallel}}\right)^{1/2} \nu, \quad (59c)$$

$$\bar{\nu}_* = \left(\frac{N}{2}\right)^{-1} \left(\frac{\gamma_{\perp}}{\gamma_{\parallel}}\right)^{1/2} \nu_*, \quad (59d)$$

$$\bar{m} = \left(\frac{N}{2}\right)^{-1} m \quad (59e)$$

with the saturation photon number defined as $n_s = \gamma_{\parallel}\gamma_{\perp}/4g^2$ and where $\bar{\alpha}_*\bar{\alpha}$ satisfies the state equation for absorptive bistability:

$$\bar{\alpha}_*\bar{\alpha}[1 + 2C/(1 + \bar{\alpha}_*\bar{\alpha})]^2 = Y^2. \quad (60)$$

Here C is the cooperativity parameter from the optical bistability literature, defined as $C = g^2N/2\kappa\gamma_{\perp}$ and Y is the scaled input driving field, $Y = \varepsilon/\kappa\sqrt{n_s}$.

A. Numerical solutions to stochastic differential equations

It is possible to solve the set of stochastic differential equations [Eq. (55e)] directly using Euler's algorithm. The solutions to the set of equations is obtained by starting the system in the deterministic steady state given by Eqs. (56). A pair of Gaussian distributed random numbers is generated by the polar method and the individual trajectories of the field variables for approximately 10^5 atomic lifetimes. The trajectories are averaged together and the running average is recorded. The parameter space that could reasonably be explored was restricted by two factors. The size of the fluctuations in the field is proportional to C , or more fundamentally, to N , the number of atoms. Roughly this is due to the fact that the field is driven by a polarization made up of N atoms. Therefore the intensity correlation function, which is fourth order in the fields, scales as N^4 . Many more trajectories must then be averaged together as N increases, if the relative error in the final result is to be kept below some chosen level such as 1%. This becomes an important factor for C on the order of 20 for the number of atoms chosen for this investigation ($N=10$). Greater values of C lead to computer runs that are prohibitively long. Various integration step sizes have been tested and checked to ensure a reliable result. One effect of using too large a step size is that the fluctuations will appear to be too large for a given set of parameters. That is, the ensemble average converges to some value that would actually correspond to a larger value of C . Of a perhaps more fundamental nature is the limit set at the opposite extreme of a small number of atoms. The stochastic differential equations are derived from a Fokker-Planck equation, a derivation rests upon the assumption that $N \gg 1$.

Several discussions have appeared in the literature concerning the limits of validity of the positive- P representation in general, and of its "pathologies" under certain integration schemes [58,59]. In our own work we have found signs of these problems; however, we have taken care to choose parameters such that runaway trajectories were not present in the running averages. Illustrations of the types and effects of unbounded trajectories on both $g^{(2)}(0)$ and $g^{(2)}(0)$ are shown in Ref. [52]. In effect, once we began to push the technique to larger values of C (on the order of 20) or to smaller values of atomic number ($N=5$), the integrations (at the least) became more unstable. An example of the results obtained from the numerical solution of the stochastic differential equations will be shown in Sec. VIII in the course of discussion of the parameter dependence of the time-dependent second-order correlation function.

B. Linearized theory

One interesting parameter regime is that in which the system is in a well defined deterministic steady state and any perturbations, quantum or otherwise, are relatively small. For example, fluctuations in the photon number in the cavity (say, when one photon escapes) is small compared to the total number of photons present. There are limits to the validity of this assumption, and in fact it will be shown later that it is precisely in the case where the fluctuations become large that the nonclassical features of interest will be found [43]. In spite of this, and because the results can be justified later and shown by other means to be at least qualitatively accurate, the small fluctuation assumption is used here as a starting point. In this situation it is valid to linearize the set of stochastic differential equations about the steady state by assuming

$$\vec{\xi} = \langle \vec{\xi} \rangle + \delta \vec{\xi}, \quad (61)$$

where

$$\vec{\xi} = (\alpha, \alpha_*, v, v_*, m)^T, \quad (62)$$

from which the set of equations can be written as

$$\frac{d(\delta \vec{\xi})}{d\tau} = -A \delta \vec{\xi} + B d\vec{\zeta}(\tau), \quad (63)$$

where A and $D = BB^T$ are the drift and diffusion matrices, respectively, and $\zeta = (0, 0, dW_1, dW_2, dW_3)^T$. The drift matrix determines the time evolution of the mean values of the variables, while the diffusion matrix is related to the fluctuations about the mean. These are given explicitly by the matrices

$$A = \begin{pmatrix} -\frac{\mu}{2}(1+i\Theta) & 0 & \frac{\mu C}{\sqrt{\Gamma}} & 0 & 0 \\ 0 & -\frac{\mu}{2}(1-i\Theta) & 0 & \frac{\mu C}{\sqrt{\Gamma}} & 0 \\ -\frac{1+\Delta^2}{2\sqrt{\Gamma}(1+\Delta^2+X^2)} & 0 & -\frac{1+i\Delta}{2\Gamma} & 0 & \frac{X}{2\sqrt{\Gamma}} \\ 0 & -\frac{1+\Delta^2}{2\sqrt{\Gamma}(1+\Delta^2+X^2)} & 0 & -\frac{1-i\Delta}{2\Gamma} & \frac{X}{2\sqrt{\Gamma}} \\ \frac{(1+i\Delta)X}{2(1+\Delta^2+X^2)} & \frac{(1+i\Delta)X}{2(1+\Delta^2+X^2)} & -\frac{X}{2\sqrt{\Gamma}} & -\frac{X}{2\sqrt{\Gamma}} & -1 \end{pmatrix} \quad (64)$$

and

$$D = -\frac{1}{N(1+\Delta^2+X^2)} \begin{pmatrix} 0 & 0 & 0 & 0 & 0 \\ 0 & 0 & 0 & 0 & 0 \\ 0 & 0 & (1-i\Delta)X^2 & -\frac{1-\Gamma}{\Gamma}X^2 & 0 \\ 0 & 0 & -\frac{1-\Gamma}{\Gamma}X^2 & (1+i\Delta)X^2 & 0 \\ 0 & 0 & 0 & 0 & -4 \end{pmatrix}, \quad (65)$$

where the scaled parameters (again from the optical bistability literature definitions) are $X = \alpha/n_s$, $\Gamma = \gamma_{\parallel}/2\gamma_{\perp}$, and $\mu = 2\kappa/\gamma_{\parallel}$. With these results it is now possible to understand various features of the N atom+cavity system.

In the case of weak intracavity field, such that the atoms are not saturated, the formalism given in the preceding section can be used to derive analytic results for the normalized second-order correlation function $g^{(2)}(\tau)$. This is possible

for a quite general choice of parameters such as the cavity and atomic detunings (Θ and Δ , respectively), as well as for an arbitrary ratio of population to polarization decay rates (given by the parameter $\Gamma = \gamma_{\parallel}/2\gamma_{\perp}$). For $\Gamma = 1$ (i.e., purely radiative decay), the results presented here are a simple generalization of Ref. [37] to include detunings and will be compared to the results of Sec. IV. When the decay of the atoms is not purely radiative, for example, due to collisions or ho-

mogeneous broadening mechanisms, the pure-state factorization described in Secs. III and IV cannot be applied. Since the stochastic dynamical model is not restricted in this sense, it is useful to calculate the correlation function here and, together with the comparisons that can be made for $\Gamma = 1$, obtain at least a qualitative feeling for the effects of nonradiative decay processes. Recent atomic beam experiments have, for example, remnant transit broadening caused by the finite interaction time of the atoms as they cross the cavity waist; this can be modeled as broadening process which effectively alters the polarization decay rate γ_{\perp} and thus Γ . To

evaluate possible experimental limitations it is important to have an estimate of the deviation from the ideal case.

C. Linearized theory in the weak-field limit

When the intracavity field is very weak compared to that needed to saturate the atoms it is possible to simplify the set of equations given in the preceding section by assuming the steady-state inversion to be constant, $\bar{m} = -1$. In this case the drift and diffusion matrices can be written as

$$A = \frac{1}{2} \begin{pmatrix} -\mu(1+i\Theta) & 0 & 2\frac{\mu C}{\Gamma} & 0 \\ 0 & -\mu(1-i\Theta) & 0 & 2\frac{\mu C}{\sqrt{\Gamma}} \\ -\frac{1+\Delta^2}{\sqrt{\Gamma}(1+\Delta^2)} & 0 & -\frac{1+i\Delta}{\Gamma} & 0 \\ 0 & -\frac{1+\Delta^2}{\sqrt{\Gamma}(1+\Delta^2)} & 0 & -\frac{1-i\Delta}{\Gamma} \end{pmatrix} \quad (66)$$

and

$$D = BB^T = -\frac{X^2}{N(1+\Delta^2)} \begin{pmatrix} 0 & 0 & 0 & 0 \\ 0 & 0 & 0 & 0 \\ 0 & 0 & 1-i\Delta & \frac{\Gamma-1}{\Gamma} \\ 0 & 0 & \frac{\Gamma-1}{\Gamma} & 1+i\Delta \end{pmatrix}. \quad (67)$$

We now have the necessary equations to investigate the photon statistics of this system.

VII. DELAYED COINCIDENCE RATES FROM STOCHASTIC DYNAMICS

The normalized second-order intensity correlation function is given in general by

$$\begin{aligned} g^{(2)}(0) &= \frac{\langle \hat{a}^{\dagger 2} \hat{a}^2 \rangle}{\langle \hat{a}^{\dagger} \hat{a} \rangle^2} \\ &= 1 + (n_s X^2 + \langle \Delta \hat{a}^{\dagger} \Delta \hat{a} \rangle)^{-2} \{ 4n_s X^2 \langle :(\Delta \hat{A}_1)^2: \rangle \\ &\quad + 2n_s^{1/2} X [\langle (\Delta \hat{a}^{\dagger})^2 \Delta \hat{a} \rangle + \text{c.c.}] + \langle (\Delta \hat{a}^{\dagger})^2 \Delta \hat{a}^2 \rangle \\ &\quad - \langle \Delta \hat{a}^{\dagger} \Delta \hat{a} \rangle^2 \} \end{aligned} \quad (68)$$

where the colons denote normal ordering and $\hat{A}_1 = \frac{1}{2}(\hat{a}^{\dagger} + \hat{a})$ is the field quadrature in phase with the driving field. The fluctuations are assumed to be Gaussian and thus the

third-order moments are zero. In contrast to Ref. [37] the higher-order (fourth order in field or of order $1/N^2$ in system ‘‘size’’) terms will not be dropped. Although this would appear to be an inconsistent treatment of the fluctuations, it will be justified later and shown *a posteriori* to be a sensible approach. These fourth-order field fluctuation correlations can be written as products of second-order correlations, which gives for weak fields

$$\lim_{X \rightarrow 0} g^{(2)}(0) = 1 + \frac{[G_{11}^0 + G_{22}^0 + 2G_{12}^0 + G_{11}^0 G_{22}^0 + G_{12}^{0,2}]}{1 + G_{12}^{0,2}}, \quad (69)$$

where G_{ij}^0 denotes the component of the correlation matrix [38] in the limit $X \rightarrow 0$, e.g., $G_{11}^0 = \lim_{X \rightarrow 0} [\langle \Delta \hat{a} \Delta \hat{a} \rangle / X^2]$. For $\Gamma = 1$ we find that $G_{12}^0 = G_{21}^0 = 0$ and by definition $G_{11}^{0*} = G_{22}^0$ so that the above may be written as

$$|1 + G_{11}^0|^2. \quad (70)$$

This simple result can be compared to that found in Ref. [42] for the correlation function of the transmitted intensity in the limit of a single atom interacting with a strongly damped resonator field mode (the ‘‘bad-cavity’’ limit in the language of the optical bistability literature). The form of the correlation function has the important property that it is bounded by zero, as must be the case. This was not so, for example, in earlier work, and the failure of the linearization was suspected to be the cause of this problem, since it arises only for very small system sizes (n_s or N small). The difference here can be simply traced to the higher-order fluctuation terms that were retained in the derivation of Eq. (68), and thus

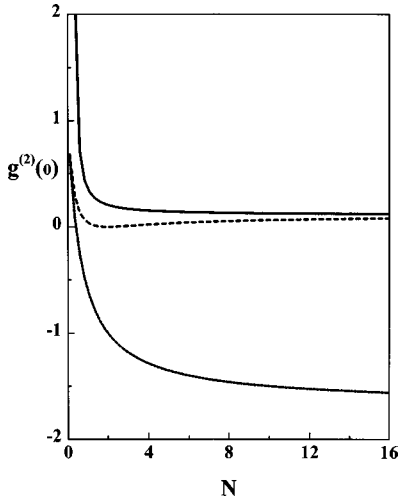


FIG. 3. $g^{(2)}(0)$ as calculated by three methods. The solid line is the pure-state theory, the dashed line is obtained from a linearized theory with second-order terms, and the dotted line is obtained from the usual linearized theory. All curves are for $g/\gamma = \kappa/\gamma = 1.0$.

provides the first justification of that assumption. This mod-squared form was found in the calculation using the pure-state formalism in the weak-field limit.

It remains now to calculate the correlation $\langle \Delta \hat{a} \Delta \hat{a} \rangle$, which is straightforward using

$$AG + GA^T = D. \quad (71)$$

The result is found to be

$$G_{11}^0 = -\frac{2\mu C^2}{\tilde{\Theta} \tilde{\Delta}^2 N} \left[\frac{C \tilde{\Theta}^*}{|\tilde{\Theta}|^2} + \frac{1}{2} \mu \tilde{\Theta} + \frac{1}{2} \tilde{\Delta} + \frac{\mu C \tilde{\Delta}^*}{|\tilde{\Delta}|^2} \right]^{-1}, \quad (72)$$

where $\tilde{\Theta} = 1 + i\Theta$ and $\tilde{\Delta} = 1 + i\Delta$. For $\Delta = \Theta = 0$ this reduces to the result of Ref. [37].

For $\Delta = \Theta = 0$ it is easier to examine the general features of the result in Eq. (72). It is important to understand the significance of the terms of order $1/N^2$ and why it is necessary to retain them. Purely from the point of view of consistency these terms should be neglected because the Fokker-Planck equation is derived including only terms of order $1/N$, and the result obtained from the linearized treatment of fluctuations must necessarily follow from that. In Fig. 3, $g^{(2)}(0)$ is plotted for various numbers of atoms when the $1/N^2$ terms are kept, and when they are not included. The exact result from the pure-state analysis is also shown. We see that by keeping these higher-order terms, $g^{(2)}(0)$ is now bounded by zero as it must be; it can be seen explicitly from the form of Eq. (70) that the minimum for the function is bounded by zero.

It is difficult to justify formally these higher-order fluctuation terms, but it can be seen that they become important only when the size of the fluctuations become comparable to the mean field itself. Naively keeping terms of the next higher order can be rationalized *a posteriori* in two ways. The first is the lower bound this sets on $g^{(2)}(\tau)$, necessary for any intensity correlation function. Second, the results so obtained agree with those found using other different meth-

ods of calculation, one of which is not based on a system size expansion. We see that there is good agreement between the linearized theory and the pure-state results for as few as 20 atoms. The agreement is even better in the good-cavity limit ($\kappa \rightarrow 0$), where the saturation photon number is quite high, and the relative size of field fluctuations is smaller.

A. General time-dependent solution in the linearized approach

It is very useful to notice that the result given by Eq. (72) is exactly that of Ref. [37] if we let $\kappa \rightarrow \kappa(1 + i\phi) = \tilde{\kappa}$ and $\gamma \rightarrow \gamma(1 + i\Delta) = \tilde{\gamma}$ (and therefore $\mu \rightarrow \tilde{\mu} = 2\tilde{\kappa}/\tilde{\gamma}$ and $C \rightarrow \tilde{C} = g^2 N / \tilde{\kappa} \tilde{\gamma}$). With this remark, and keeping in mind the modulus square form of the correlation function ($\Gamma = 1$), the full time-dependent second-order intensity correlation function can be written simply, following Ref. [37] as

$$g^{(2)}(\tau) = \left| 1 - \frac{2\tilde{C}}{N} \frac{\tilde{\mu}}{\tilde{\mu} + 1} \frac{2\tilde{C}}{1 + 2\tilde{C}} e^{-(1/4)(\tilde{\mu} + 1)\tau} \right. \\ \left. \times \left[\cosh \tilde{\Omega} \tau + \frac{\tilde{\mu} + 1}{4\tilde{\Omega}} \sinh \tilde{\Omega} \tau \right] \right|^2, \quad (73)$$

where

$$\tilde{\Omega} = \left[\frac{1}{16} (\tilde{\mu} - 1)^2 - \frac{1}{2} \tilde{\mu} \tilde{C} \right]^{1/2}. \quad (74)$$

This differs from the result of the pure state formalism in the factor of

$$2\tilde{C}/(1 + 2\tilde{C}) \neq 2\tilde{C}/(1 + 2\tilde{C} - 2\tilde{C}_1). \quad (75)$$

In the limit of large N , the two solutions are the same. It is expected that there could only be agreement for this case, as a large number of atoms is implicit in the linearization of the stochastic model. The nature of the agreement seems to validate the inclusion of higher-order terms in the linearization procedure. The Fokker-Planck equation was derived with an assumption of ‘‘large’’ system size, i.e., N large, and particularly in the limit of large quantum noise, $\mu \gg 1$, this could be predicted to lead to a lack of confidence in the formalism. It is somewhat surprising that the deviations from the pure-state formalism are fairly small and in any case only quantitative in nature. Such a result gives a certain degree of confidence that when the next generalization is made, to allow for nonradiative decay ($\Gamma \neq 1$), the linearized treatment can be regarded as a good approximation as long as it is not pushed to extremes.

B. Linearized theory and Gaussian factorization

The question of the validity of the linearized theory approach with higher-order terms will be addressed now by making a comparison to the pure-state formalism approach. Since no system size truncation was made in the derivation of the results in Sec. IV, that will be used as our reference for the comparison. We have already shown that the correlation function can be expressed as

$$g^{(2)}(0) = |\langle g|\hat{a}^2|\phi_{ss}\rangle|^2 |\langle g|\hat{a}|\phi_{ss}\rangle|^4. \quad (76)$$

If we write $\hat{a} = \langle \hat{a} \rangle + \Delta \hat{a}$ then

$$g^{(2)}(0) = \left| 1 + \frac{\langle \Delta a^2 \rangle}{\langle \hat{a} \rangle^2} \right|^2, \quad (77)$$

where, again, only weak fields have been considered, thus justifying the replacement of $\langle g|$ by $\langle \phi_{ss}|$.

Now we will see if this result is obtained using the linearized theory with the Gaussian factorization theorem for the fluctuations. Using the general definition of $g^{(2)}(0)$ and the decomposition of \hat{a} we can write

$$g^{(2)}(0) = \frac{\langle \hat{a}^{\dagger 2} \hat{a}^2 \rangle}{\langle \hat{a}^{\dagger} \hat{a} \rangle^2} \quad (78)$$

and after some rearranging

$$g^{(2)}(0) = \frac{\left| 1 + \frac{\langle \Delta a^2 \rangle}{\langle \hat{a} \rangle^2} \right|^2 + \frac{\langle \Delta a^{\dagger 2} \Delta a^2 \rangle - \langle \Delta a^{\dagger 2} \rangle \langle \Delta a^2 \rangle}{\langle \hat{a}^{\dagger} \rangle^2 \langle \hat{a} \rangle^2} + 4 \frac{\langle \Delta a^{\dagger} \Delta a \rangle}{\langle \hat{a}^{\dagger} \rangle \langle \hat{a} \rangle}}{\left(1 + \frac{\langle \Delta a^{\dagger} \Delta a \rangle}{\langle \hat{a}^{\dagger} \rangle \langle \hat{a} \rangle} \right)^2}. \quad (79)$$

For weak fields $\langle \Delta a^{\dagger} \Delta a \rangle / \langle \hat{a}^{\dagger} \rangle \langle \hat{a} \rangle \ll 1$ and if the Gaussian factorization theorem is invoked to reduce the fourth-order correlations to products of second-order correlations giving

$$\langle \Delta a^{\dagger 2} \Delta a^2 \rangle = \langle \Delta a^{\dagger 2} \rangle \langle \Delta a^2 \rangle.$$

Equation (79) then reduces to Eq. (77). This agreement will be the strongest justification for retaining the terms that were in previous work neglected; in fact, presented in this fashion

it is natural to keep the extra term as being consistent with the definition of $g^{(2)}(0)$. We see here as well that the terms of fourth order become important for a situation in which the mean square field fluctuations are large and the mean field itself is small, exactly where one expects to see large non-classical effects in the photon statistics of the light transmitted by the cavity.

The complete time dependent solution is given formally by

$$g^{(2)}(\tau) = \frac{1 + 2 \operatorname{Re}(G_{11}^0(\tau)) + G_{12}^0(\tau)G_{21}^0(\tau) + |G_{11}^0(\tau)|^2 + |G_{12}^0(\tau)|^2}{1 + 2 \operatorname{Re}(G_{12}^0(0)) + |G_{12}^0(0)|^2}, \quad (80)$$

where

$$G_{ij}(\tau) = \frac{G_{ij}^0}{2\Omega} \left[\left[-\frac{\mu}{2}(1+i\Theta) + \frac{\mu}{\sqrt{\Gamma}} + \frac{1}{2} \frac{1+i\Delta}{\Gamma} \right] \sinh \Omega \tau + 2\Omega \cosh \Omega \tau \right] \exp \left[-\frac{1}{4} \left(\frac{1+i\Delta}{\Gamma} + \mu(1+i\Theta) \right) \right] \quad (81)$$

with G_{ij} as defined in conjunction with Eq. (69).

As mentioned earlier, for purposes of comparison to experiment the general expression including detunings and nonradiative decay processes is necessary. For $\Delta, \Theta = 0$ and $\Gamma = 1$, $g^{(2)}(\tau)$ is a perfect square,

$$g^{(2)}(\tau) = |1 + G_{11}(\tau)|^2, \quad (82)$$

as in the pure-state case.

The frequency Ω is the imaginary part of the eigenvalue describing the time-dependent response of the coupled atom-cavity system. As was discussed in the Introduction, this has

been referred to as the ‘‘vacuum field Rabi frequency’’ and represents the exchange frequency for excitation between the atomic polarization and the cavity field.

VIII. PARAMETER DEPENDENCE

In this section we will examine the behavior of $g^{(2)}(0)$ and $g^{(2)}(\tau)$ as a function of the various rates and detunings, as well as the number of atoms. Figure 3 shows the dependence of $g^{(2)}(0)$ on the number of atoms N . Generally, we find that the linearized theory does quite well for $N = 10$ – 100 atoms. The agreement is best in the good-cavity limit, as there the photon number is generally larger, and an alternate system size expansion in terms of photon number would be a good approximation. In Fig. 4, we examine photon antibunching in the system, defined as $g^{(2)}(0) < 1$. The effect here is that $g^{(2)}(0)$ is actually independent of the number of atoms and still exhibits large amounts of antibunching; it is possible to have ‘‘perfect’’ anticoincidence, $g^{(2)}(0) = 0$ for an arbitrarily large number of atoms. Recall that for zero detunings, the pure-state result

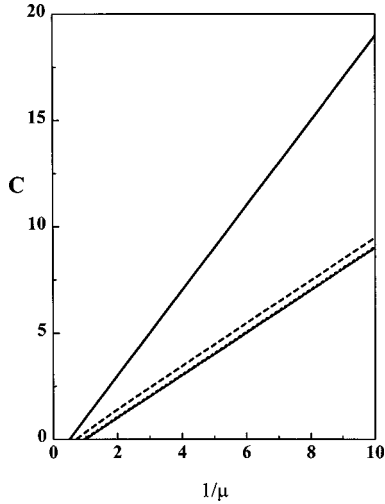


FIG. 4. The solid line indicates the locus of points for which $g^{(2)}(0)=0.0$. The region between the other lines and the solid line indicate the regions where $g^{(2)}(0)<1$, photon antibunching. The dashed line is for $N=1$, and the dotted line is for $N=10$. The curve for $N=100$ lies on top of the one for $N=10$.

$$g^{(2)}(0) = \frac{[(1+2C)(1-2C'_1)]^2}{1+2C-2C'_1}. \quad (83)$$

We see that there is perfect antibunching so long as $2C'_1 = 1$. As this quantity is independent of the number of atoms, we can have perfect antibunching for an arbitrary number of atoms. What is the meaning of this condition? In terms of fundamental rates, we have

$$2C'_1 = \frac{g^2}{(\gamma/2)(\kappa + \gamma/2)} = \frac{g^2/(\kappa + \gamma/2)}{(\gamma/2)}. \quad (84)$$

The numerator of $2C'_1$ is the spontaneous emission rate into the cavity mode, and the denominator $\gamma/2$ is the spontaneous emission rate out the sides of the cavity. When these rates are equal, half of the spontaneous emission goes into the cavity mode, and we have perfect antibunching. In terms of the fraction of spontaneous emission into the cavity mode,

$$\beta = \frac{2C'_1}{1+2C'_1}, \quad (85)$$

this condition can be expressed as $\beta=0.5$. Physically this is when the polarization in the collapsed state is equal in magnitude and opposite in sign to the driving field, for a zero mean intercavity field. This leads to a null detection of the second photon.

In Fig. 4, the solid line represents the locus of points (in terms of C_1 and $1/\mu$) for which $g^{(2)}(0)=0$, perfect antibunching. The other curves indicate regions of parameter space where $g^{(2)}(0)<1$. These regions are above and to the left of the dashed curves, and are presented for $N=1, 10$, and 100.

The space of cavity and atomic detunings will be considered next. As we move from the bad-cavity ($\mu \rightarrow \infty$) limit to the good-cavity ($\mu \rightarrow 0$) limit the relative importance of atomic and cavity detunings changes dramatically. In the

former case, Fig. 5(a), there is very little sensitivity in the size of the observable nonclassical effect to the cavity detuning Θ ; even at $\Theta=2$ there is negligible change. At the same time, for $\Delta=2$ there are no nonclassical correlations any longer; in fact the full time-dependent correlation shows that $g^{(2)}(\tau)$ for this case exhibits photon bunching, or excess correlations for large Δ . When $\kappa=\gamma$, Fig. 5(b), we see that either a detuning of $\Delta=\gamma/2$ or $\Theta=\kappa$ is very deleterious to the antibunching. Finally, when γ is larger than κ , the antibunching is most easily destroyed by detuning the atoms.

In the special case of $\mu=1$, and equal and opposite detunings, we see that the presence of detuning may actually enhance the antibunching, until the detuning becomes larger than the level widths. This is exhibited in Fig. 5(c). When we discuss the time-dependent correlation function we will see

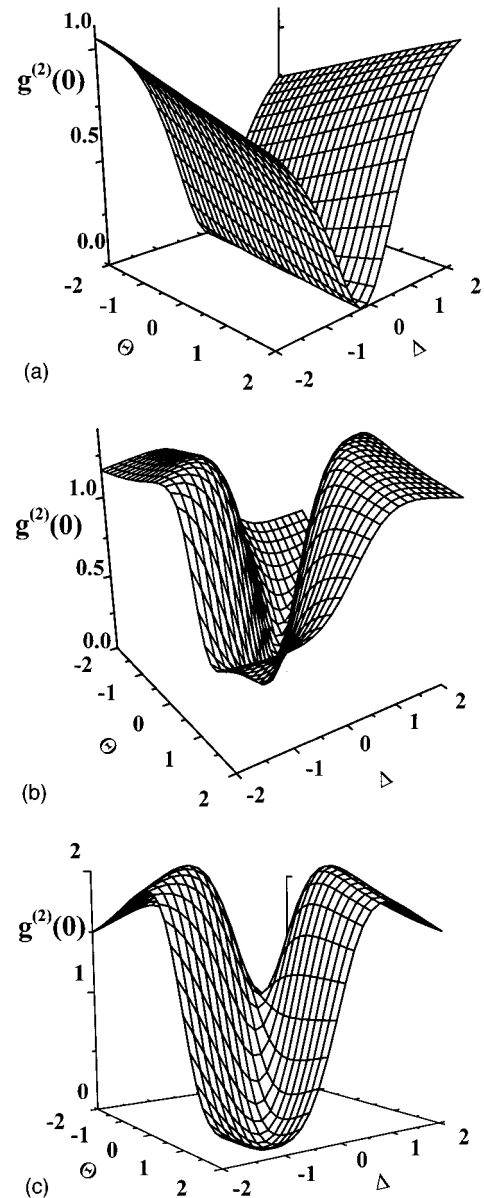


FIG. 5. (a) Surface plot of $g^{(2)}(0)$ vs atomic and cavity detunings for $g/\gamma=2.29$, $\kappa/\gamma=10$, and $N=100$. (b) Surface plot of $g^{(2)}(0)$ vs atomic and cavity detunings for $g/\gamma=0.866$, $\kappa/\gamma=1.0$, and $N=100$. (c) Surface plot of $g^{(2)}(0)$ vs atomic and cavity detunings for $g/\gamma=1.0$, $\kappa/\gamma=0.5$, and $N=100$.

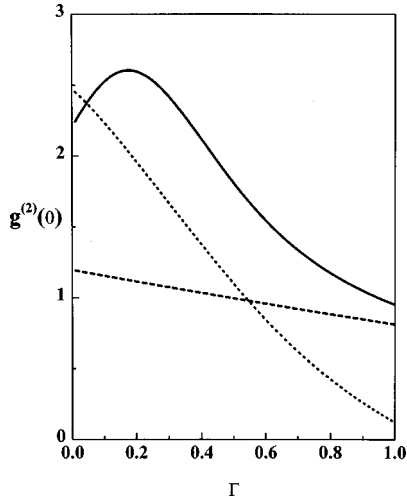


FIG. 6. $g^{(2)}(0)$ vs Γ for $g/\gamma=0.158$, $N=20$, and (solid line) $\kappa/\gamma=5.0$, (dashed line) $\kappa/\gamma=0.5$, and (dotted line) $\kappa/\gamma=0.05$.

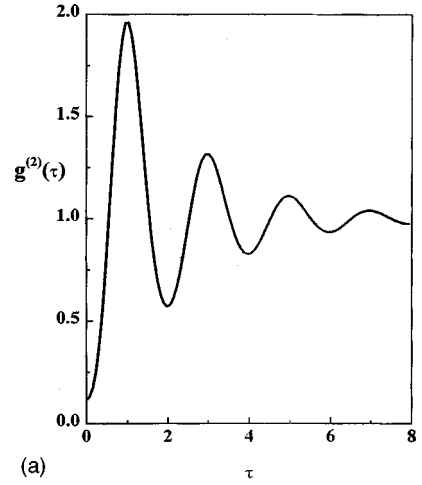
the resolution to this seeming contradiction which allows for a “larger” nonclassical effect with detunings. Effectively there are different types of nonclassical correlation possible, two of which are competing in the case discussed here. The number of atoms has little effect on the dependence of “loss” of nonclassical character with detuning. It tends to be true that larger N will lead to less sensitivity on the cavity detuning, but it is in general the case that the nonclassical effects are less sensitive to the cavity than to atomic detunings.

The last parameter of interest is Γ , which is equal to 1 for purely radiative broadening and 0 in the limit of purely transit time broadening. We see from Fig. 6 that transit time broadening severely limits the antibunching, and may indeed lead to bunching instead. This is to be expected as the root of the effect is the interference between the driving field and the field radiated by the atom. Transit time broadening will essentially smear out the atomic phase, erasing the interference effects.

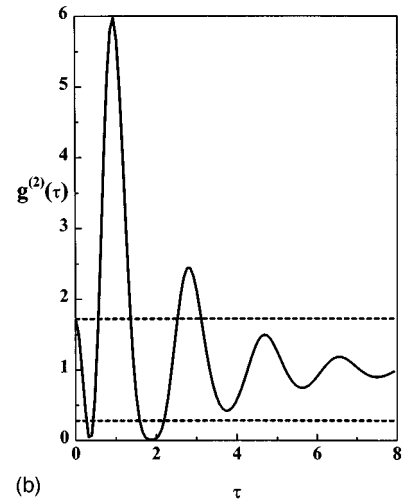
We now turn our attention to the time dependent $g^{(2)}(\tau)$. Figure 7 illustrates three different cases in which nonclassical photon correlations appear. In Fig. 7(a) we see $g^{(2)}(0) < 1$ and $g^{(2)}(\tau) \geq g^{(2)}(0)$. The temporal behavior is very similar to that observed in single-atom resonance fluorescence but it should be emphasized once more that in this case the field is very weak compared to that needed to saturate the atomic transition, and the oscillation frequency is independent of the field strength; this is not the case for single-atom resonance fluorescence, where the Rabi oscillations predicted theoretically and observed experimentally are a function of the driving field, $\Omega_R \propto |E|^2$. Here, the oscillation frequency is determined by the collective coupling parameter $\sqrt{N}g$, a manifestation of vacuum-Rabi oscillations.

In Fig. 7(b) the time dependent correlation function starts at $\tau=0$ at a value $2 > g^{(2)}(0) > 1$ then decreases to zero at some finite time delay τ' . From the Cauchy-Schwarz inequality it can be shown that for a classical stochastic process [60]

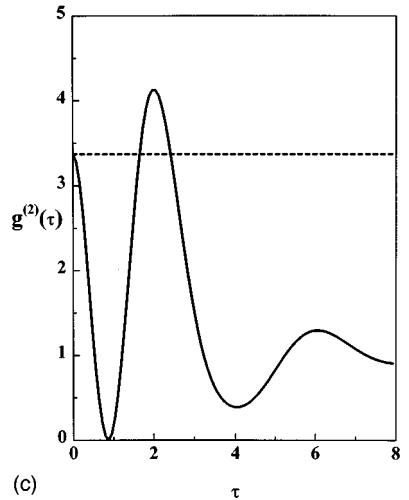
$$\langle \bar{I}(t)\bar{I}(t+\tau) \rangle \leq \langle \bar{I}(t)^2 \rangle. \quad (86)$$



(a)



(b)



(c)

FIG. 7. (a) $g^{(2)}(\tau)$ vs τ for $g/\gamma=0.577$, $\kappa/\gamma=0.5$, and $N=30$. (b) $g^{(2)}(\tau)$ vs τ for $g/\gamma=1.06$, $\kappa/\gamma=0.5$, and $N=10$. The region between the dashed lines denotes the allowed values of the correlation function for a classical field. (c) $g^{(2)}(\tau)$ vs τ for $g/\gamma=1.10$, $\kappa/\gamma=0.5$, and $N=2$. The region below the dashed line denotes the allowed values of the correlation function for a classical field.

Written in terms of intensity fluctuations about a mean, it is possible to write

$$|g^{(2)}(\tau) - 1| \leq |g^{(2)}(0) - 1|. \quad (87)$$

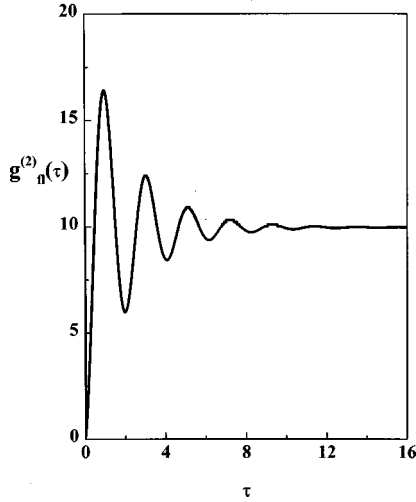


FIG. 8. $g^{(2)}(\tau)$ vs τ for the fluorescent field for $g/\gamma = 1.06$, $\kappa/\gamma = 0.5$, and $N = 1$.

Therefore since $g^{(2)}(0) \leq 2$ the observed behavior in Fig. 7(b) is in violation of the classical inequality for all τ for which $|g^{(2)}(\tau)| \geq g^{(2)}(0)$.

We also see that the large peak in Fig. 7(b) around $\tau = 1$ is nonclassical, as $g^{(2)}(\tau) - 1 > g^{(2)}(0) - 1$. Further, in Fig. 7(c), we see that the peak in $g^{(2)}(\tau)$ around $\tau = 2.5$ is nonclassical, but the zero in $g^{(2)}(\tau)$ near $\tau = 1$ is not. We refer to values of $g^{(2)}(\tau)$ in excess of those allowed classically as overshoots, and undershoots are defined as $g^{(2)}(\tau)$ values below that allowed classically. This overshoot has recently been observed by Mielke, Foster, and Orozco [45]. A complete discussion of the nonclassical nature of the behavior was given by Rice and Carmichael in the context of a single atom in the bad-cavity limit [42], and generalized by Carmichael, Brecha, and Rice to the many-atom case [43]. The interpretations there included self-homodyning of squeezed dipole radiation with the driving field, or alternatively quantum interference of the driving field and the polarization after the collapse of the wave function upon detection of the first photon. In order to demonstrate that it is indeed an interference between the coherent driving field and the field radiated by the atom that is responsible for this effect, we plot in Fig. 8 the correlation function $g^{(2)}(\tau)$ for the fluorescent light, for the case of a single atom. We see that $g^{(2)}(\tau)$ for the fluorescent light vanishes at zero delay time, as the atom cannot simultaneously emit two photons; this is just the antibunching seen in resonance fluorescence, here with a cavity enhanced rate for relaxation to the steady state. There are no subsequent zeros in this correlation function for any choice of C_1 . Increasing the number of atoms only decreases the antibunching, essentially proportional to $1 - 1/N$ as in resonance fluorescence; there still appear no zeros at subsequent times.

In Fig. 9 is shown a progression of curves as the number of atoms is varied from 1 to 100. As N (and therefore C) is increased the value of $g^{(2)}(0)$ is seen to show only a weak dependence, as was to be expected. For $N \approx 10$ there is virtually no change in the zero time delay correlation. There is a greater change in the excess correlation seen for a finite time delay, and there is as well a larger number of multiple zeros or points at which, for a finite time delay there is zero

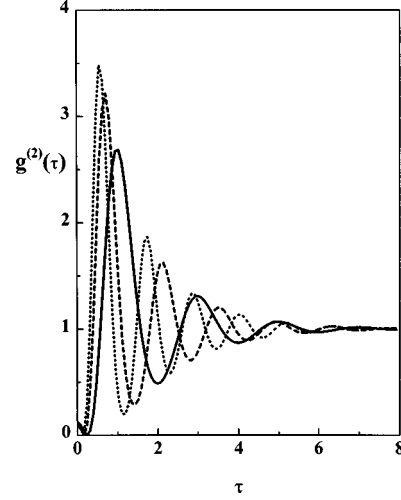


FIG. 9. $g^{(2)}(\tau)$ vs τ for $g/\gamma = \kappa/\gamma = 1.0$, with (solid line) $N = 1$, (dashed line) $N = 10$, and (dotted line) $N = 100$.

probability of there being a second photon emitted from the cavity. Essentially, as expected, for large g there is no N dependence in $g^{(2)}(0)$, but for small coupling strengths this is no longer the case. In the oscillatory regime, there is some N dependence, in that the vacuum-Rabi frequency depends on the number of atoms. The size of $\Delta\alpha/\alpha$ is independent of the number of atoms for large N and/or large g , and is on the order of unity, but the number of zeros in $g^{(2)}(\tau)$ will depend on the vacuum-Rabi frequency.

In the strong coupling regime, as seen above, $g^{(2)}(\tau)$ may oscillate many times before relaxing to unity. In this regime, it is found that it is possible to have several zeroes in $g^{(2)}(\tau)$. This is exhibited in Figs. 10(a)–10(b). The interpretation of this is exactly the same as in the bad-cavity limit. Recall that this mean field is the superposition of the coherent driving field and the out of phase polarization field. In the bad-cavity limit, we found that as the mean field relaxed to its steady-state value it passed through zero, and at this time a second photon could not be emitted, leading to a zero in $g^{(2)}(\tau)$ at a nonzero delay time. In the oscillatory regime, the only new feature is that relaxation to the steady state is oscillatory, leading to the possibility of multiple zeroes in $g^{(2)}(\tau)$ at a variety of delay times. Due to the simple form of $g^{(2)}(\tau)$, it is easy to construct a map in $C - 1/\mu$ space to denote the number of zeroes in $g^{(2)}(\tau)$. We may write

$$g^{(2)}(\tau) = [1 + |c_a| (e^{\lambda\tau + i\phi} + e^{\lambda^*\tau - i\phi})]^2. \quad (88)$$

The derivative of $g^{(2)}(\tau)$ is given by

$$g^{(2)'}(\tau) = 2[1 + |c_a| (e^{\lambda\tau + i\phi} + e^{\lambda^*\tau - i\phi})] \times \{ |c_a| [\lambda e^{\lambda\tau + i\phi} + \lambda^* e^{\lambda^*\tau - i\phi}] \}. \quad (89)$$

We see that we may have a simultaneous zero in $g^{(2)}(\tau)$ and its first derivative under the condition

$$2|c_a| \exp\{[\lambda_r/\lambda_i][(2l+1)\pi - 2\phi]\} = 1, \quad (90)$$

where λ_i and λ_r are the real and imaginary parts of λ . We may, for a particular value of l , pick a value of C_1 and use

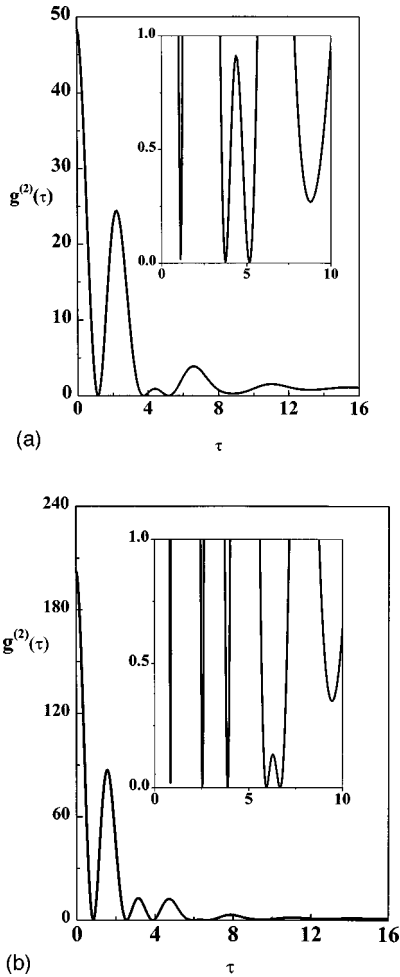


FIG. 10. (a) $g^{(2)}(\tau)$ vs τ for $g/\gamma=1.44$, $\kappa/\gamma=0.138$, and $N=1$. (b) $g^{(2)}(\tau)$ vs τ for $g/\gamma=2.04$, $\kappa/\gamma=0.278$, and $N=1$.

Eq. (90) to find the value of $1/\mu$ at which another new zero appears in $g^{(2)}(\tau)$. The result is a series of curves in $C - 1/\mu$ space that denote the appearance of another zero in $g^{(2)}(\tau)$. For a fixed C , decreasing $1/\mu$ below the value on one of the curves results in a correlation function with a pair of zeroes very close together, as $g^{(2)}(\tau)$ ‘‘bounces’’ off the time axis. The region above and to the left of the rightmost curve in Fig. 11 indicates the region where there is always a zero in $g^{(2)}(\tau)$. The next curve to the left indicates where a second zero appears. To the immediate left and above this curve there are three zeros. Subsequent curves denote the appearance of a new pair of zeroes, which are degenerate on the curve, but split into a pair of zeroes to the left and above the curve. Increasing the number of atoms increases the vacuum-Rabi frequency ($\sqrt{N}g$), and therefore for a larger number of atoms, the relaxation to steady state occurs at a higher frequency leading to more zeroes in $g^{(2)}(\tau)$.

With detunings added, we must consider a complicated solution so we will now proceed to some pictures. In Fig. 12(a), for $2\kappa=\gamma=g$ we show $g^{(2)}(\tau)$ for $\Delta=0.5$ and $\Theta=0.0$. We see that detunings on the order of half the linewidth is deleterious to the nonclassical effects. The dip to zero is gone, and in fact the undershoot is gone as well. The overshoots that follow are still present, but are reduced. These disappear fully when the detuning is on the order of a

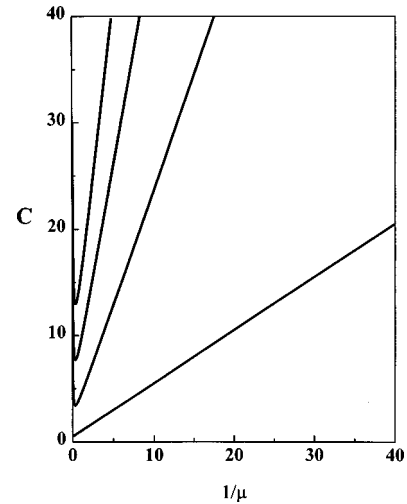


FIG. 11. Successive appearance of zeroes in $g^{(2)}(\tau)$. The left-most curve indicates where $g^{(2)}(0)=0.0$. To the left of this curve one zero appears in $g^{(2)}(\tau)$ at some delay time. Each additional curve indicates where another pair of zeroes appears.

linewidth. In order to understand this sensitivity, we examine a parametric plot of the real and imaginary parts of the quantity whose squared magnitude yields $g^{(2)}(\tau)$. This would be $1 + \text{Re}(\Delta\alpha/\alpha)$ and $\text{Im}(\Delta\alpha/\alpha)$. The singular nature of the zeroes in $g^{(2)}(\tau)$ is evident when we realize that both the real and imaginary parts of this quantity must simultaneously be zero for $g^{(2)}(\tau)$ to be zero. For zero detuning, the imaginary part is zero, and the trajectory of the parametric plot repeatedly passes through zero, if $\Delta\alpha/\alpha$ is large enough. When detunings are introduced, the parametric explores the complex plane. This is due simply to the beating of the polarization field and the driving field, as they no longer oscillate at the same frequency. For a detuning of $\Delta=0.5$ and $\Theta=0.0$ [Fig. 12(a)], the trajectory is always significantly away from $(-1,0)$, the place corresponding to $g^{(2)}(\tau)=0$.

For equal detunings, $\Delta=\Theta=0.5$, Figs. 12(c), nearly all nonclassical effects are absent, and the trajectory does not oscillate along a line, but more of a cuspy figure that rarely passes near zero for tunings along the order of half a linewidth.

When we consider equal and opposite detunings, with $\mu=1$, we find the surprising result that the nonclassical behavior remains, and indeed we now have antibunching where there was bunching for zero detunings, as seen earlier. In Fig. 12(e), we see that the nonclassical behavior persists in time. Mathematically, this stems from the fact that for this situation, the complex vacuum-Rabi frequency is still completely imaginary, and so the overall decay constant of $\Delta\alpha/\alpha$ is not too much different than in the case of nonzero detunings. Physically, with equal and opposite detunings, the states $|0+\rangle$ and $|1-\rangle$ are equally split above and below the laser field.

In the good-cavity limit, characterized by a cavity linewidth that is narrow compared to the atomic linewidth, the size of nonclassical effects, such as antibunching, are small. A plot of $g^{(2)}(\tau)$ in this limit is exhibited in Fig. 13(a). This limit is characterized by a large saturation number n_s , and as such the usual linearized small noise theory should apply, and in fact the pure-state and linearized results are nearly

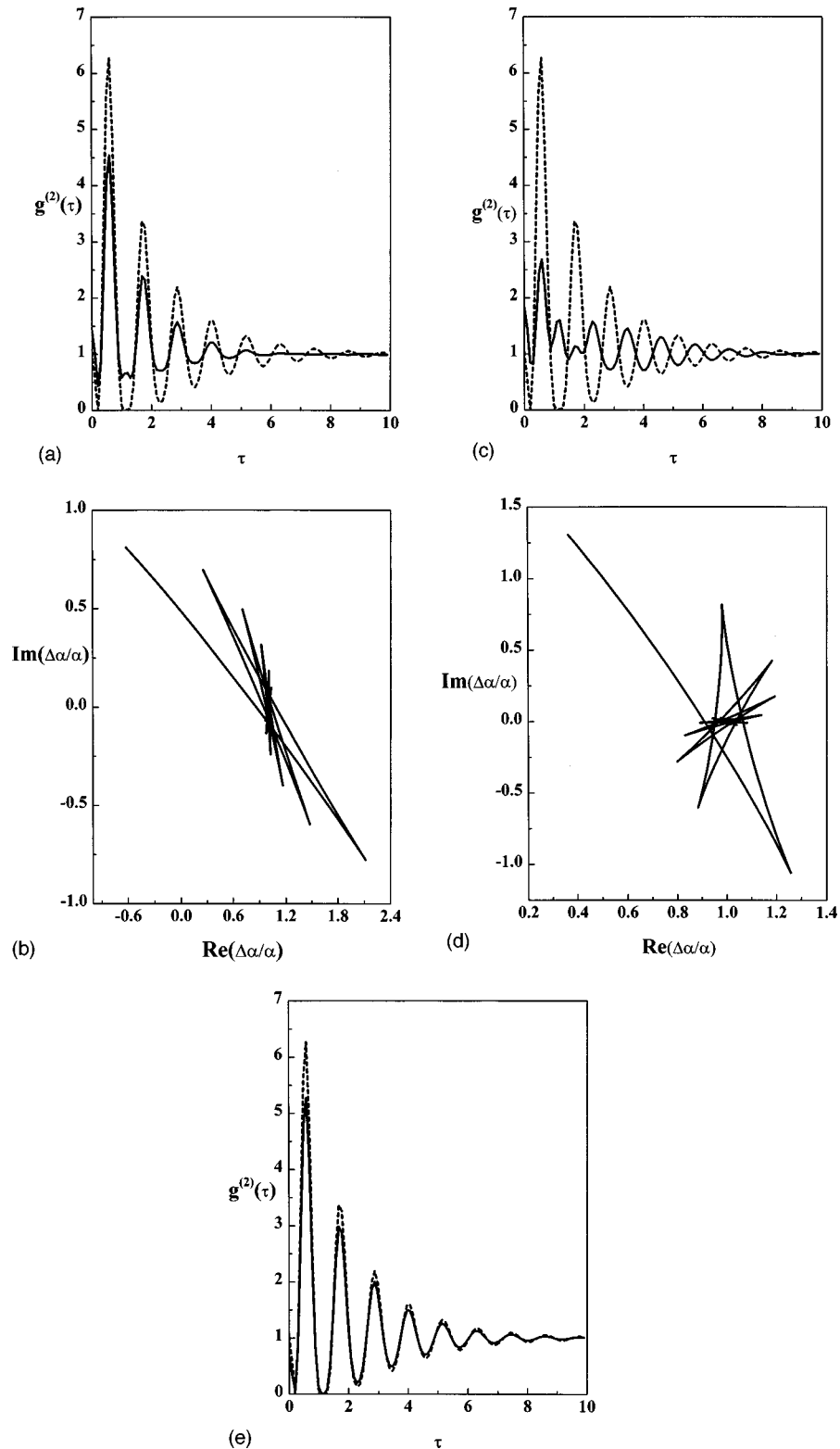


FIG. 12. (a) $g^{(2)}(\tau)$ vs τ for $g/\gamma=1.0$, $\kappa/\gamma=0.5$, and $N=30$. The solid line is for $\Delta=0.5$ and $\Theta=0.0$ and dashed line is for zero detunings. (b) Parametric plot of $\Delta\alpha/\alpha$ for $g/\gamma=1.0$, $\kappa/\gamma=0.5$, and $N=30$, $\Delta=0.5$, and $\Theta=0.0$. (c) $g^{(2)}(\tau)$ vs τ for $g/\gamma=1.0$, $\kappa/\gamma=0.5$, and $N=30$. The solid line is for $\Delta=0.5$ and $\Theta=0.5$ and the dashed line is for zero detunings. (d) Parametric plot of $\Delta\alpha/\alpha$ for $g/\gamma=1.0$, $\kappa/\gamma=0.5$, and $N=30$, $\Delta=0.5$, and $\Theta=0.5$. (e) $g^{(2)}(\tau)$ vs τ for $g/\gamma=1.0$, $\kappa/\gamma=0.5$, and $N=30$. The solid line is for $\Delta=0.5$ and $\Theta=-0.5$ and the dashed line is for zero detunings.

identical. In this limit, quantum fluctuations are a small perturbation on the semiclassical steady state, and there is little departure from coupled oscillator results based on a semiclassical analysis. It takes many photons to effect a change in

response of the system, and so quantum noise is not as important in this limit as in other parameter regimes. It is obvious that the linearized theory works well here.

In the bad-cavity limit, Fig. 13(b), nonclassical effects can

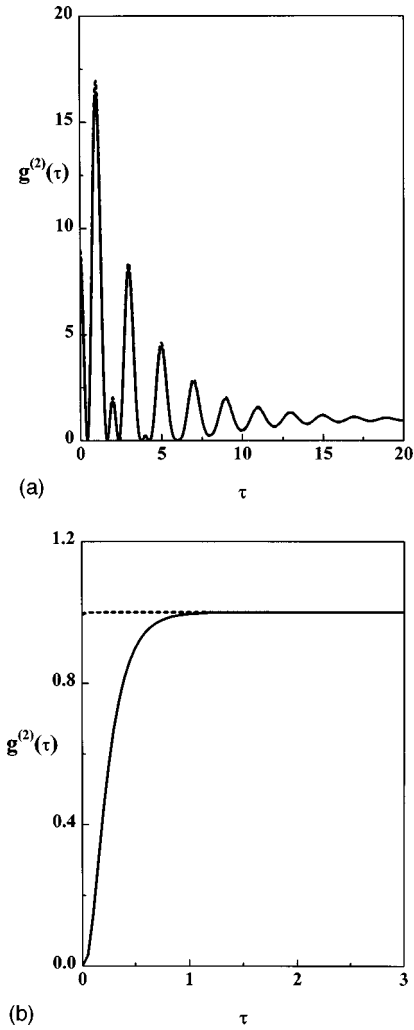


FIG. 13. (a) $g^{(2)}(\tau)$ vs τ for $g/\gamma=1.0$, $\kappa/\gamma=0.01$, and $N=1$. The solid line is for the pure state theory and the dashed line is the result of the linearized theory. (b) $g^{(2)}(\tau)$ vs τ for $g/\gamma=5.0$, $\kappa/\gamma=50.0$, and $N=100$. The solid line is for the pure state theory and the dashed line is the result of the linearized theory.

be quite dramatic; perfect antibunching, for example. In the bad-cavity limit, the saturation photon number is much less than 1, hence one photon has a big effect on the system dynamics. In this regime, quantum fluctuations are quite important, and the linearized theory is quite inadequate. Indeed, for Fig. 13(b), we see that the linearized theory predicts less than 0.1% antibunching, while the true result is maximal antibunching $g^{(2)}(0)=0.0$. Results obtained here agree with the results of Rice and Carmichael by adiabatic elimination of the field.

Finally, the case of nonradiative decay of the atoms will be considered. For $\Gamma \neq 1$ the amount of nonclassical correlations decreases as a function of increasing homogeneous broadening. We investigate the effect of transit broadening on the nonclassical correlations by considering the result of this mechanism to be an increased transverse decay rate γ_{\perp} . Thus Γ , which has until now always been taken equal to unity for the time-dependent correlations, will be taken as a parameter to be varied. In practice it will be defined by the geometry of the system and it is desirable to keep it as near unity (purely radiative broadening) as possible.

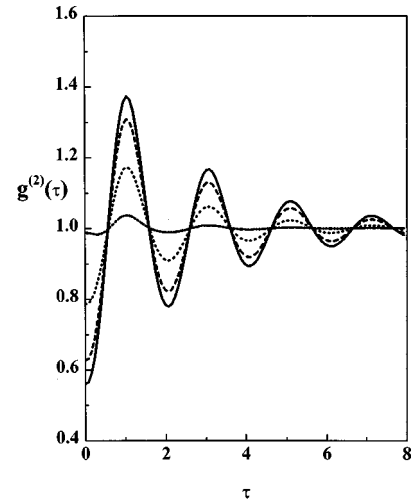


FIG. 14. $g^{(2)}(\tau)$ vs τ for $g/\gamma=0.31$, $\kappa/\gamma=0.5$, and $N=100$. These are presented for (solid line) $\Gamma=1.0$, (dashed line) $\Gamma=0.9$, (dotted line) $\Gamma=0.7$, and (short-dashed line) $\Gamma=0.5$.

In Fig. 14 is shown the time-dependent correlation function for parameters similar to those of recent experiments, with each curve representing a different value of Γ . From this it is apparent that it is desirable to allow the atoms to interact with the cavity field for a time long compared to the atomic lifetime and thus eliminate transit broadening. The obvious solution to this problem is to use atoms that have been either cooled or even trapped. Recently two groups have demonstrated the feasibility of dropping cooled atoms through a cavity, which makes the transit time broadening completely negligible [61,62].

An example of the results of the stochastic differential equation numerical solution discussed in Sec. VI is shown in Fig. 15. Parameters are chosen to be similar to those of recent experiments by Foster *et al.*; in our notation the relevant values are $N=10$, $C=10$, and $\mu=1$. The qualitative agreement between the SDE results and those of the pure-state theory and the linearized theory (also shown on the plot as a dashed curve) is very good.

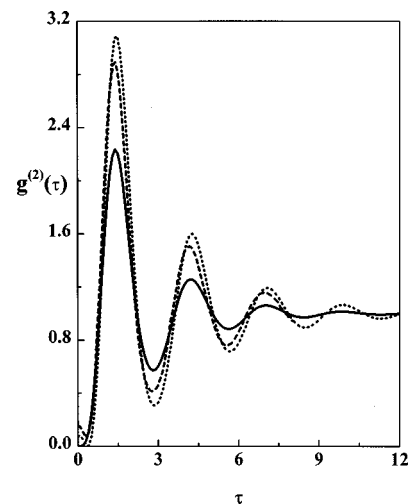


FIG. 15. A comparison of the (solid line) pure state theory, (dashed line) linearized theory with higher order terms, and (dotted line) simulations of the stochastic differential equations in Eq. (64). The parameters are $g/\gamma=0.7071$, $\kappa/\gamma=0.5$, and $N=10$.

IX. CONCLUSION

In this work we have examined the nonclassical photon statistics of the N -atom/cavity system, with atomic and cavity decay, and a classical driving field. These include $g^{(2)}(0) < 1$ and a positive slope for $g^{(2)}(\tau)$ at $t=0$, as well as the vanishing of $g^{(2)}(\tau)$ for a nonzero delay time. The nonclassical effects are essentially independent of the number of atoms for large N , and thus persist for macroscopic systems. The nonclassical behavior occurs when the ‘‘cavity QED condition,’’ $(\bar{\gamma} - \gamma)/\gamma \approx 1$, is fulfilled, and are thus dynamical rather than structural in nature. That is, these cavity QED effects are beyond simple modifications of linewidths and lineshapes.

We have given the formal procedure behind the pure-state formalism used in previous work [43], which holds even though we consider a dissipative system and we have discussed the physical reasons for the effectiveness of this approach. We have discussed the nonclassical behavior of this system in terms of quantum interference of probability amplitudes. It is found that in the good-cavity limit ($\gamma \gg \kappa$), the nonclassical behavior is small, while in the bad-cavity limit ($\kappa \gg \gamma$), nonclassical fluctuations are quite prominent. This is understood in terms of the saturation photon number, which is large in the good-cavity limit, and small in the bad-cavity limit. In the latter case, a single photon changes the behavior of the system appreciably, and hence quantum fluctuations play an important role in determining system dynamics. In the good-cavity limit, small fluctuations of one or two photons do not appreciably alter the system, hence the limitation of the size of the nonclassical effect. The nonclassical effect is extremely sensitive to atomic and cavity detunings; detunings of approximately half of the respective linewidths will seriously affect the nonclassical effect. This has been explained in a graphical manner. This has serious implications for experimental realizations of this model, making the precise locking of atomic and cavity resonances paramount.

We have also examined a stochastic model for this system that goes beyond the normal quantum theory of optical bistability in that higher-order fluctuations are considered. The treatment is justified *a posteriori* by the agreement of this stochastic model with results of the pure-state formalism, as well as a Gaussian factorization ansatz.

It is useful to compare the different theoretical approaches taken in this paper. This will serve to identify the limitations as well as the strengths of each. First, perhaps the most complete model is that provided by the stochastic differential equations. The rigorous numerical solution of these equations has the limitation of becoming cumbersome for large numbers of atoms, and at the same time, of being limited at the other extreme of small atom number by linearization assumptions. The analytical linearized theory presented here has the same limitation for small atom numbers, however, we find in both cases that even $N \approx 5$ allows for at least a qualitatively correct solution, as compared to the pure-state formalism. The linearized theory (with the inclusion of higher-order fluctuation terms) allows for a reasonable comparison of theory to experiment, since in all experiments to date, transit-broadening-induced polarization decay must be accounted for. The pure-state formalism does not allow for

this to be done. The ‘‘justification’’ of the linearized theory with the addition of $1/N^2$ terms (inconsistent with the original derivation of the Fokker-Planck equation in the positive- P representation) is found by a comparison with the pure-state formalism in the limit of no transit broadening ($\Gamma = 1$). The agreement between this stochastic model and the results of the pure-state formalism is striking even for $N = 5$; this is surprising as the limit $N \rightarrow \infty$ is taken in the stochastic model.

The conclusion to be drawn from all of these results is that the Fokker-Planck equation approach, although using the assumption of a large number of atoms, can be used with some confidence for this system even with a relatively small N . This is of some use because even though the pure-state result is exact and compact, it is restricted to the purely radiatively broadened case. For $\Gamma \neq 1$, the linearized theory can be used to make predictions, and to compare to experimental results or $N = 10$ –100 atoms.

ACKNOWLEDGMENT

The authors would like to express their deepest gratitude to Howard Carmichael, without whose guidance this work would not have been possible.

APPENDIX A: DENSITY MATRIX ELEMENT EQUATIONS IN THE WEAK-FIELD LIMIT

We begin with the master equation (6) written out in full:

$$\begin{aligned} \dot{\rho} = & g \left(\hat{a}^\dagger \sum_j \sigma_-^j - \hat{a} \sum_j \sigma_+^j \right) \rho - g \rho (\hat{a}^\dagger \sum_j \sigma_-^j - \hat{a} \sum_j \sigma_+^j) \\ & + E(\hat{a}^\dagger - \hat{a})\rho - E\rho(\hat{a}^\dagger - \hat{a}) + (\gamma/2)[\sum_j 2\sigma_-^j \rho \sigma_+^j - \sum_j \sigma_-^j \rho \\ & - \rho \sum_j \sigma_+^j - N\rho] + \kappa(2\hat{a}\rho\hat{a}^\dagger - \hat{a}^\dagger\hat{a}\rho - \rho\hat{a}^\dagger\hat{a}). \end{aligned} \quad (A1)$$

For the field, we use the usual Fock state basis

$$|0\rangle \quad |1\rangle \quad |2\rangle. \quad (A2)$$

For the atoms, we use the states

$$\begin{aligned} |0\rangle_A &= |;-N/2\rangle, \\ |1\rangle_A &= |k;-N/2+1\rangle, \\ |2\rangle_A &= |k,l;-N/2+2\rangle. \end{aligned} \quad (A3)$$

The labels $-N/2, -N/2+1, -N/2+2$ denote the inversion eigenvalues for these states, and the labels (k,l) denote which atom is in the excited state if any, and (k,l) can separately take on any value from 1 to N , the total number of atoms. In terms of atomic states for individual atoms, these become

$$\begin{aligned} |;-N/2\rangle &= \prod_j |-\rangle_j, \\ |k;-N/2+1\rangle &= \prod_j |-\rangle_j |+\rangle_k \prod_j |-\rangle_j, \end{aligned} \quad (A4)$$

$$|k,l;-N/2+2\rangle = \prod_j |-\rangle_j |+\rangle_k \prod_j |-\rangle_j |+\rangle_l \prod_j |-\rangle_j.$$

These states correspond, respectively, to 0, 1, and 2 excited atoms. Now our combined basis set, truncated at the two-photon level in keeping with our desire to obtain results in the weak-field limit, is

$$\begin{aligned}
&|0\rangle|;-N/2\rangle, \\
&|1\rangle|;-N/2\rangle, \\
&|0\rangle|k;-N/2+1\rangle, \\
&|2\rangle|;-N/2\rangle, \\
&|1\rangle|k;-N/2+1\rangle, \\
&|0\rangle|k,l;-N/2+2\rangle.
\end{aligned} \tag{A5}$$

Again, here the first state corresponds to zero quanta excitation, the following two correspond to two quanta of excitation, and the last three correspond to three quanta of excitation. There are $1+(N+1)+(N(N-1)+N+1)=N^2+N+3$ states in this basis. However, since the atoms are assumed to be identical, and to interact with the field via the same coupling strength g , one can greatly reduce the number of density matrix elements that must be considered. Essentially, we only need keep track of the states with both k and l labels, and there will be several cases that are distinct, corresponding to $k=l$ or $k\neq l$. We consider a few examples here:

$$\langle 0|\langle;-N/2|\rho|0\rangle|k,l;-N/2+2\rangle \tag{A6}$$

are all identical for all l and k , and

$$\langle 2|\langle;-N/2|\rho|0\rangle|k,l;-N/2+2\rangle \tag{A7}$$

are all equal for all k so long as l is not equal to k . So here, we have two cases to consider, where $k=l$, and $k\neq l$. So we label our density matrix elements in the following manner:

$$\rho_{n,m;j,k}=\langle n|_A\langle m|\rho|j\rangle|k\rangle_A. \tag{A8}$$

Here, we have 28 independent density matrix elements, with 21 coming from the fact that we have essentially a six-state basis, and an additional seven coming from the keeping track of k and l . For example, consider the matrix elements

$$\begin{aligned}
&\langle 1|\langle k;-N/2+1|\rho|1\rangle|l(l\neq k);-N/2+1\rangle, \\
&\langle 1|\langle k;-N/2+1|\rho|1\rangle|l(l=k);-N/2+1\rangle.
\end{aligned} \tag{A9}$$

These two matrix elements are not equal in general, and to simplify our notation, we shall refer to them as $\rho_{1,1;1,1}^u$, and $\rho_{1,1;1,1}^l$, respectively. All other density matrix elements that are not uniquely defined by the subscripts will carry the u or l distinctions, for like and unlike atoms, respectively. The only exception will be the following two-photon matrix elements,

$$\begin{aligned}
\rho_{02;02}^{ll} &= \langle 0|\langle k,l;-N/2+2|\rho|1\rangle|k,l;-N/2+2\rangle, \\
\rho_{02;02}^{lu} &= \langle 1|\langle k,l;-N/2+2|\rho|1\rangle \\
&\quad \times |k,m(m\neq l), \text{ or } m,l(m\neq k);-N/2+2\rangle,
\end{aligned} \tag{A10}$$

$$\begin{aligned}
\rho_{02;02}^{uu} &= \langle 1|\langle k,l;-N/2+2|\rho|1\rangle \\
&\quad \times |m,l(m\neq k), \text{ or } n,l(n\neq k);-N/2+2\rangle.
\end{aligned}$$

We must now examine the equations of motion of these density matrix elements, using the master equation (6). We arrive at

$$\begin{aligned}
\dot{\rho}_{00;00} &= -2E\rho_{00;10} + N\gamma\rho_{01;01}^l + 2\kappa\rho_{10;10}, \\
\dot{\rho}_{00;10} &= Ng\rho_{00;01} - E\rho_{10;10} - \sqrt{2}E\rho_{00;20} + N\gamma\rho_{01;11}^l + 2\sqrt{2}\kappa\rho_{10;20} - \kappa\rho_{00;10} + E\rho_{00;00}, \\
\dot{\rho}_{00;01} &= -g\rho_{00;10} - E\rho_{10;01} - E\rho_{00;11} + (N-1)\gamma - E\rho_{01;01}^l - (\gamma/2)\rho_{00;01} + 2\kappa - E\rho_{10;11}, \\
\dot{\rho}_{00;20} &= \sqrt{2}Ng\rho_{00;11} - E\rho_{10;20} + \sqrt{2}E\rho_{00;10} - 2\kappa\rho_{00;20}, \\
\dot{\rho}_{00;11} &= -\sqrt{2}g\rho_{00;20} + (N-1)g\rho_{00;02} - E\rho_{10;11} + E\rho_{00;01} - (\gamma/2 + \kappa)\rho_{00;11}, \\
\dot{\rho}_{00;02} &= -2g\rho_{00;11} - E\rho_{10;02} - \gamma\rho_{00;02}, \\
\dot{\rho}_{10;10} &= 2Ng\rho_{10;01} + E\rho_{00;10} - 2\sqrt{2}E\rho_{20;10} + E\rho_{00;10} + N\gamma\rho_{11;11}^l + 4\kappa\rho_{20;20} - 2\kappa\rho_{10;10}, \\
\dot{\rho}_{10;01} &= (N-1)g\rho_{01;01}^u + g(\rho_{01;01}^l - \rho_{10;10}) - \sqrt{2}E\rho_{01;20} - E\rho_{10;11} + N\gamma\rho_{11;02}^l - (\gamma/2 + \kappa)\rho_{10;01} + 2\sqrt{2}\kappa\rho_{20;11} + E\rho_{00;01}, \\
\dot{\rho}_{10;20} &= (N-1)g\rho_{01;20}^u + g\rho_{01;20}^l + \sqrt{2}Ng\rho_{10;11} + E\rho_{00;20} - \sqrt{2}E(\rho_{20;20} - \rho_{10;10}) - 3\kappa\rho_{10;20} + \sqrt{2}Ng\rho_{10;11}, \\
\dot{\rho}_{10;11} &= (N-1)g\rho_{01;11}^u + g\rho_{01;11}^l - \sqrt{2}g\rho_{10;20} + (N-1)g\rho_{10;02} + E(\rho_{00;11} + \rho_{10;01}) - \sqrt{2}E\rho_{20;11} - (\gamma/2 + 2\kappa)\rho_{10;11}, \\
\dot{\rho}_{10;02} &= (N-2)g\rho_{01;02}^u + 2g\rho_{01;02}^l - 2g\rho_{10;11} + E\rho_{00;02} - \sqrt{2}E\rho_{20;02} - (\gamma + \kappa)\rho_{10;02}, \\
\dot{\rho}_{01;01}^l &= -2g\rho_{10;01} - 2E\rho_{11;01}^l + (N-1)\rho_{02;02}^{ll} - \gamma\rho_{01;01}^l + 2\kappa\rho_{11;11}^l,
\end{aligned} \tag{A11}$$

$$\begin{aligned}
\dot{\rho}_{01;01}^u &= -2g\rho_{10;01} - 2E\rho_{11;01}^u + (N-2)\rho_{02;02}^{lu} - \gamma\rho_{01;01}^u + 2\kappa\rho_{11;11}^u, \\
\dot{\rho}_{01;20} &= -g\rho_{10;20} + (N-1)\sqrt{2}g\rho_{01;11}^u + \sqrt{2}g\rho_{01;11}^l - E\rho_{11;20} + \sqrt{2}E\rho_{01;10} - (\gamma/2 + 2\kappa)\rho_{01;20}, \\
\dot{\rho}_{01;11}^l &= -g\rho_{10;11} - \sqrt{2}g\rho_{01;20} + (N-1)g\rho_{01;02}^l - E(\rho_{11;11}^l - \rho_{01;01}^l) - (\gamma + \kappa)\rho_{01;11}^l, \\
\dot{\rho}_{01;11}^u &= -g\rho_{10;11} - \sqrt{2}g\rho_{01;20} + g\rho_{01;02}^l + (N-2)g\rho_{01;02}^u - E(\rho_{11;11}^u - \rho_{01;01}^u) - (\gamma + \kappa)\rho_{01;11}^u, \\
\dot{\rho}_{01;02}^l &= -g\rho_{10;02} - g\rho_{01;11}^l - g\rho_{01;11}^u - E\rho_{11;02}^l - (3\gamma/2)\rho_{01;02}^l, \\
\dot{\rho}_{01;02}^u &= -g\rho_{10;02} - 2g\rho_{01;11}^u - E\rho_{11;02}^u - (3\gamma/2)\rho_{01;02}^u, \\
\dot{\rho}_{20;20} &= 2\sqrt{2}Ng\rho_{20;11} + 2\sqrt{2}E\rho_{10;20} - 4\kappa\rho_{20;20}, \\
\dot{\rho}_{20;11} &= \sqrt{2}Ng\rho_{11;11} - \sqrt{2}g\rho_{20;20} + (N-1)g\rho_{20;02} + \sqrt{2}E\rho_{10;11} - (\gamma/2 + 3\kappa)\rho_{20;11} + E\rho_{01;20}, \\
\dot{\rho}_{20;02} &= \sqrt{2}(N-2)g\rho_{11;02}^u + 2\sqrt{2}g\rho_{11;02}^l + \sqrt{2}E\rho_{10;02} - (\gamma + 2\kappa)\rho_{20;02}, \\
\dot{\rho}_{11;11}^l &= -2\sqrt{2}g\rho_{20;11} + 2(N-1)g\rho_{11;02}^l + 2E\rho_{01;11}^l - (\gamma + 2\kappa)\rho_{11;11}^l, \\
\dot{\rho}_{11;11}^u &= -2\sqrt{2}g\rho_{20;11} + 2g\rho_{11;02}^l + 2(N-2)g\rho_{11;02}^u + 2E\rho_{01;11}^u - (\gamma + 2\kappa)\rho_{11;11}^u, \\
\dot{\rho}_{11;02}^l &= g\rho_{02;02}^{lu} + g(N-2)\rho_{02;02}^{lu} - \sqrt{2}g\rho_{20;02} + g(N-2)\rho_{20;02} - g(\rho_{11;11}^l + \rho_{11;11}^u) + E\rho_{01;02}^l - (3\gamma/2 + \kappa)\rho_{11;02}^l, \\
\dot{\rho}_{11;02}^u &= 2g\rho_{02;02}^{lu} + g(N-3)\rho_{02;02}^{uu} - \sqrt{2}g + g(N-2)\rho_{20;02} - 2g\rho_{11;11}^u + E\rho_{01;02}^u - (3\gamma/2 + \kappa)\rho_{11;02}^u, \\
\dot{\rho}_{02;02}^{ll} &= -4g\rho_{11;02}^l - 2\gamma\rho_{02;02}^{ll}, \\
\dot{\rho}_{02;02}^{lu} &= -2g\rho_{11;02}^l - 2g\rho_{11;02}^u - 2\gamma\rho_{02;02}^{lu}, \\
\dot{\rho}_{02;02}^{uu} &= -4g\rho_{11;02}^u - 2\gamma\rho_{02;02}^{uu}.
\end{aligned}$$

We now scale time in units of the atomic lifetime γ , and introduce the scaling ansatz

$$\rho_{n,l;m,k} \rightarrow n_s^{(n+m)/2} Y^{(n+m+l+k)} \rho_{n,l;m,k}. \quad (\text{A12})$$

Keeping only terms to lowest order in Y , we have the following set of equations:

$$\begin{aligned}
\dot{\rho}_{00;00} &= 0, \\
\dot{\rho}_{00;10} &= \sqrt{2}\mu C\rho_{00;10} - (\mu/2)\rho_{00;10} - (\mu/2)\rho_{00;00}, \\
\dot{\rho}_{00;01} &= -1/2\sqrt{2}\rho_{00;10} - (1/2)\rho_{00;01}, \\
\dot{\rho}_{00;20} &= 2\mu C\rho_{00;11} + (\mu/\sqrt{2})\rho_{00;10} - \mu\rho_{00;20}, \\
\dot{\rho}_{00;11} &= -(1/2)\rho_{00;20} + \sqrt{2}\mu C(1-1/N)\rho_{00;02} + \mu/2\rho_{00;01} - (1/2)(1+\mu)\rho_{00;11}, \\
\dot{\rho}_{00;02} &= -(1/\sqrt{2})\rho_{00;11} - (1/2)\rho_{00;02}, \\
\dot{\rho}_{10;10} &= 2\sqrt{2}\mu C\rho_{10;01} + \mu\rho_{00;10} - \mu\rho_{10;10}, \\
\dot{\rho}_{10;01} &= \sqrt{2}\mu C(1-1/N)\rho_{01;01}^u + \sqrt{2}\mu C/N\rho_{01;01}^l - (1/2\sqrt{2})\rho_{10;10} + \mu/2\rho_{00;01} - (1/2)(1+\mu)\rho_{10;01}, \\
\dot{\rho}_{10;20} &= \sqrt{2}\mu C\rho_{01;20}^u + 2\mu C\rho_{10;11}^l + (\mu/2)\rho_{00;20} - (3\mu/2)\rho_{10;20} + (\mu/\sqrt{2})\rho_{10;10},
\end{aligned}$$

$$\begin{aligned}
\dot{\rho}_{10;11} &= \sqrt{2}\mu C(1-1/N)\rho_{01;11}^u + \sqrt{2}\mu C/N\rho_{01;11}^l - (1/2)\rho_{10;20} + \sqrt{2}\mu C(1-1/N)\rho_{10;02} + (\mu/2)(\rho_{10;01} + \rho_{00;11}) - \sqrt{2}E\rho_{20;11} \\
&\quad - (1/2)(1+2\mu)\rho_{10;11}, \\
\dot{\rho}_{10;02} &= \sqrt{2}\mu C(1-2/N)\rho_{01;02}^u + 2\sqrt{2}\mu C\rho_{01;02}^l + (\mu/2)\rho_{00;02} - (1+\mu/2)\rho_{10;02} - (1\sqrt{2})\rho_{10;11}, \\
\dot{\rho}_{01;01}^l &= -(1/\sqrt{2})\rho_{10;01} - \rho_{01;01}^l, \\
\dot{\rho}_{01;01}^u &= -(1/\sqrt{2})\rho_{10;01} - \rho_{01;01}^u, \\
\dot{\rho}_{01;20} &= -(1/2\sqrt{2})\rho_{10;20} + 2\mu C(1-1/N)\rho_{01;11}^u + 2\mu C\rho_{01;11}^l + (\mu/\sqrt{2})\rho_{01;10} - (1/2)(1+2\mu)\rho_{01;20}, \tag{A13} \\
\dot{\rho}_{01;11}^l &= -(1/2\sqrt{2})\rho_{10;11} - (1/2)\rho_{01;20} + \sqrt{2}\mu C(1-1/N)\rho_{01;02}^l + (\mu/2)\rho_{01;01}^l - (1+\mu/2)\rho_{01;11}^l, \\
\dot{\rho}_{01;11}^u &= -(1/2\sqrt{2})\rho_{10;11} - (1/2)\rho_{01;20} + (\sqrt{2}\mu C/N)\rho_{01;02}^l + \sqrt{2}\mu C(1-2/N)\rho_{01;02}^u + (\mu/2)\rho_{01;01}^u - (1+\mu/2)\rho_{01;11}^u, \\
\dot{\rho}_{01;02}^l &= -(1/2\sqrt{2})\rho_{10;02} - (1/2\sqrt{2})\rho_{01;11}^l - (1/2\sqrt{2})\rho_{01;11}^u - (3/2)\mu\rho_{01;02}^l, \\
\dot{\rho}_{01;02}^u &= -(1/2\sqrt{2})\rho_{10;02} - (1/\sqrt{2})\rho_{01;11}^u - (3/2)\mu\rho_{01;02}^u, \\
\dot{\rho}_{20;20} &= 4\mu C\rho_{20;11} + \sqrt{2}\mu\rho_{10;20} - 2\mu\rho_{20;20}, \\
\dot{\rho}_{20;11} &= 2\mu C\rho_{11;11} - (1/2)\rho_{20;20} + \sqrt{2}\mu C(1-1/N)\rho_{20;02} + (\mu/\sqrt{2})\rho_{10;11} + (\mu/2)\rho_{01;20} - (1/2)(1+3\mu)\rho_{20;11}, \\
\dot{\rho}_{20;02} &= \mu C(1-2/N)\rho_{11;02}^u + 4\mu C/N\rho_{11;02}^l - (1/\sqrt{2})\rho_{20;11} + (\mu/\sqrt{2})\rho_{10;02} - (1+\mu)\rho_{20;02}, \\
\dot{\rho}_{11;11}^l &= -\rho_{20;11} + 2\sqrt{2}\mu C(1-1/N)\rho_{11;02}^l + \mu\rho_{01;11}^l - (1+\mu)\rho_{11;11}^l + \mu\rho_{01;11}^u, \\
\dot{\rho}_{11;11}^u &= -\rho_{20;11} + (2\sqrt{2}\mu C/N)\rho_{11;02}^l + 2\sqrt{2}\mu C(1-2/N)\rho_{11;02}^u - (1+\mu)\rho_{11;11}^u, \\
\dot{\rho}_{11;02}^l &= \sqrt{2}\mu C/N\rho_{02;02}^u + \sqrt{2}\mu C(1-2/N)\rho_{02;02}^u - (1/2)\rho_{20;02} - (1/\sqrt{2})\rho_{11;11}^u - (1/2\sqrt{2})\rho_{11;11}^l + (\mu/2)\rho_{01;02}^u \\
&\quad - (1/2)(3+\mu)\rho_{11;02}^u, \\
\dot{\rho}_{11;02}^u &= 2\sqrt{2}\mu C/N\rho_{02;02}^u + \sqrt{2}\mu C(1-3/N)\rho_{02;02}^u - (1/2)\rho_{20;02} - (1/\sqrt{2})(\rho_{11;11}^l + \rho_{11;11}^u) + (\mu/2)\rho_{01;02}^l - (1/2)(3+\mu)\rho_{11;02}^l, \\
\dot{\rho}_{02;02}^l &= -\sqrt{2}\rho_{11;02}^l - 2\rho_{02;02}^l, \\
\dot{\rho}_{02;02}^u &= -(1/\sqrt{2})(\rho_{11;02}^l + \rho_{11;02}^u) - 2\rho_{02;02}^u, \\
\dot{\rho}_{02;02}^{uu} &= -\sqrt{2}\rho_{11;02}^u - 2\rho_{02;02}^{uu}.
\end{aligned}$$

At this point, we construct equations of motion for quantities such as $\Delta\rho_{n,m;k,l} = (\rho_{n,m;k,l}^l - \rho_{n,m;k,l}^u)$. Rather than write down more equations, we simply state the result. The differences between like and unlike atom density matrix elements are coupled only to each other. Hence, if we start from an initial ground state, where the differences are zero initially, they remain zero for all times. For the rest of our analysis, we restrict ourselves to this scenario, and drop the distinction between like and unlike atom density matrix elements. This is the result one would obtain if the atomic basis were initially chosen as the symmetric collective state, reflecting the permutation symmetry of the atoms. We wish to point out that these quantities couple only to one another in the weak-field limit. For example in the equation for $\Delta\rho_{01;01}$ there is a term proportional to $\rho_{02;02}^{ll}$, and hence the differences are *not* coupled only to each other, but this term is dropped in the weak-field limit as it is of order Y^4 , whereas $\rho_{01;01} = \rho_{01;01}^l = \rho_{01;01}^u$ are of order Y^2 . Setting $\rho_{n,m;k,l}^l = \rho_{n,m;k,l}^u$, as well as $\rho_{n,m;k,l}^{ll} = \rho_{n,m;k,l}^{uu} = \rho_{n,m;k,l}^{lu}$ leaves us with 21 independent density matrix elements, equivalent to those obtained by the six-state basis

$$|00\rangle |10\rangle |01\rangle |20\rangle |11\rangle |02\rangle. \tag{A14}$$

The equations of motion for the respective density matrix elements are given below:

$$\dot{\rho}_{00;00} = 0,$$

$$\begin{aligned}
\dot{\rho}_{00;10} &= \sqrt{2}\mu C\rho_{00;01} - (\mu/2)\rho_{00;10} + (\mu/2)\rho_{00;00}, \\
\dot{\rho}_{00;01} &= -1/2\sqrt{2}\rho_{00;10} - (1/2)\rho_{00;01}, \\
\dot{\rho}_{00;20} &= 2\mu C\rho_{00;11} + (\mu/\sqrt{2})\rho_{00;10} - \mu\rho_{00;20}, \\
\dot{\rho}_{00;11} &= -(1/2)\rho_{00;20} + \sqrt{2}\mu C(1-1/N)\rho_{00;02} + \mu/2\rho_{00;01} - (1/2)(1+\mu)\rho_{00;11}, \\
\dot{\rho}_{00;02} &= -(1/\sqrt{2})\rho_{00;11} - (1/2)\rho_{00;02}, \\
\dot{\rho}_{10;10} &= 2\sqrt{2}\mu C\rho_{10;01} + \mu\rho_{00;10} - \mu\rho_{10;10}, \\
\dot{\rho}_{10;01} &= \sqrt{2}\mu C\rho_{01;01} + (1/2\sqrt{2})\rho_{10;10} + \mu/2\rho_{00;01} + (1/2)(1+\mu)\rho_{10;01}, \\
\dot{\rho}_{10;20} &= \sqrt{2}\mu C\rho_{01;20} + 2\mu C\rho_{01;11} + (\mu/2)\rho_{00;20} - (3\mu/2)\rho_{10;20} + (\mu/\sqrt{2})\rho_{10;10}, \\
\dot{\rho}_{10;11} &= \sqrt{2}\mu C(1-1/N)\rho_{01;11} - \sqrt{2}\mu C/N\rho_{01;11} - (1/2)\rho_{10;20} + \sqrt{2}\mu C(1-1/N)\rho_{10;02} + (\mu/2)(\rho_{10;01} + \rho_{00;11}) \\
&\quad - \sqrt{2}E\rho_{20;11} - (1/2)(1+2\mu)\rho_{10;11}, \\
\dot{\rho}_{10;02} &= \sqrt{2}\mu C(1-2/N)\rho_{01;02} + \sqrt{2}\mu C\rho_{01;02} + (\mu/2)\rho_{00;02} - (1+\mu/2)\rho_{10;11}, \\
\dot{\rho}_{01;01} &= -(1/\sqrt{2})\rho_{10;01} - \rho_{01;01}, \\
\dot{\rho}_{01;20} &= -(1/2\sqrt{2})\rho_{10;20} + 2\mu C\rho_{01;11} + (\mu/\sqrt{2})\rho_{01;10} - (1/2)(1+2\mu)\rho_{01;20}, \\
\dot{\rho}_{01;11} &= -(1/2\sqrt{2})\rho_{10;11} - (1/2)\rho_{01;20} + \sqrt{2}\mu C(1-1/N)\rho_{01;02} + (\mu/2)\rho_{01;01} - (1+\mu/2)\rho_{01;11}, \\
\dot{\rho}_{01;02} &= -(1/2\sqrt{2})\rho_{10;02} - (1/\sqrt{2})\rho_{01;11} - (3/2)\mu\rho_{01;02}, \\
\dot{\rho}_{20;20} &= 4\mu C\rho_{11;11} + \sqrt{2}\mu\rho_{10;20} - \rho_{20;20} - 2\mu\rho_{20;20}, \\
\dot{\rho}_{20;11} &= 2\mu C\rho_{11;11} - (1/2)\rho_{20;20} + \sqrt{2}\mu C(1-1/N)\rho_{20;02} + (\mu/\sqrt{2})\rho_{10;11} + (\mu/2)\rho_{01;20} - (1/2)(1+3\mu)\rho_{20;11}, \\
\dot{\rho}_{20;02} &= \sqrt{2}\mu C\rho_{11;02} - (1/\sqrt{2})\rho_{20;11} + (\mu/\sqrt{2})\rho_{10;02} - (1+\mu)\rho_{20;02}, \\
\dot{\rho}_{11;11} &= -\rho_{20;11} + 2\sqrt{2}\mu C(1-1/N)\rho_{11;02} + \mu\rho_{01;11} - (1+\mu)\rho_{11;11}, \\
\dot{\rho}_{11;02} &= \sqrt{2}\mu C(1-1/N)\rho_{02;02} - (1/2)\rho_{20;02} - (1/\sqrt{2})\rho_{11;11} + (\mu/2)\rho_{01;02} - (1/2)(3+\mu)\rho_{11;02}, \\
\dot{\rho}_{02;02} &= -\sqrt{2}\rho_{11;02} - 2\rho_{02;02}.
\end{aligned} \tag{A15}$$

APPENDIX B: QUANTUM THEORY OF COUPLED HARMONIC OSCILLATORS

In this appendix, we show that a pair of coherently driven, damped, coupled harmonic oscillators evolves from an initial vacuum state into the product state $|\alpha_0(t), \beta_0(t)\rangle$, where $\alpha_0(t)$ and $\beta_0(t)$ are coherent state amplitudes that satisfy the oscillator equations one would write down classically. One way to prove this is to use the Glauber-Sudarshan representation to convert the master equation

$$\begin{aligned}
\dot{\rho} &= -i\omega_a[\hat{a}^\dagger\hat{a}, \rho] - i\omega_b[\hat{b}^\dagger\hat{b}, \rho] + g[(\hat{a}^\dagger\hat{b} - \hat{b}^\dagger\hat{a}), \rho] \\
&\quad + \mathcal{E}[(\hat{a}^\dagger - \hat{a}), \rho] + \kappa_a(2\hat{a}\rho\hat{a}^\dagger - \hat{a}^\dagger\hat{a}\rho - \rho\hat{a}^\dagger\hat{a}) \\
&\quad + \kappa_b(2\hat{b}\rho\hat{b}^\dagger - \hat{b}^\dagger\hat{b}\rho - \rho\hat{b}^\dagger\hat{b})
\end{aligned} \tag{B1}$$

into a Fokker-Planck equation.

The essential point is that the resulting Fokker-Planck equation has no diffusion terms. For the initial P function where both oscillators are in the vacuum state,

$$P(\alpha, \beta, 0) = \delta^{(2)}(\alpha)\delta^{(2)}(\beta), \tag{B2}$$

the solution to the Fokker-Planck equation is

$$P(\alpha, \beta, t) = \delta^{(2)}(\alpha - \alpha_0(t))\delta^{(2)}(\beta - \beta_0(t)), \tag{B3}$$

where $\alpha_0(t)$ and $\beta_0(t)$ satisfy the equations

$$\dot{\alpha}_0 = -(\kappa_a + i\omega_a)\alpha_0 + g\beta_0 + \mathcal{E}, \tag{B4}$$

$$\dot{\beta}_0 = -(\kappa_b + i\omega_b)\beta_0 + g\alpha_0. \quad (\text{B5})$$

These are the semiclassical equations that one obtains by approximating the atom as a simple harmonic oscillator (via the Schwinger representation) upon factorization of equations of motion for expectation values. These equations will reproduce all of the structural effects of cavity QED (i.e., linewidth and level shifts), but as we have shown, they do

not reproduce the dynamical effects seen in the photon statistics. If the system is modeled as a pair of coherently driven coupled harmonic oscillators, both the field and the atom would evolve into coherent states with amplitudes that satisfy semiclassical equations of motion, and hence $g^{(2)}(\tau) = 1$ for all delay times. Hence there would be no nonclassical effects such as photon antibunching, sub-Poisson behavior, or the vanishing of $g^{(2)}(\tau)$ at a finite delay time.

-
- [1] E.M. Purcell, Phys. Rev. **69**, 681 (1946).
 [2] K.H. Drexhage, J. Lumin. **1**, 693 (1970).
 [3] R.G. Hulet, E.S. Hilfer, and D. Kleppner, Phys. Rev. Lett. **55**, 2137 (1985).
 [4] A.V. Vaidyanathan, W.P. Spencer, and D. Kleppner, Phys. Rev. Lett. **47**, 1592 (1981).
 [5] P. Goy, J.M. Raimond, M. Gross, and S. Haroche, Phys. Rev. Lett. **50**, 1903 (1983).
 [6] W. Jhe, A. Anderson, E.A. Hinds, D. Meschede, L. Moi, and S. Haroche, Phys. Rev. Lett. **58**, 666 (1987).
 [7] D.J. Heinzen, J.J. Childs, J.E. Thomas, and M.S. Feld, Phys. Rev. Lett. **58**, 1320 (1987).
 [8] O. J. Heinzen and M. S. Feld, Phys. Rev. Lett. **59**, 2623 (1987).
 [9] P. Stehle, Phys. Rev. A **2**, 102 (1970).
 [10] E.A. Power and T. Thirunamachandran, Phys. Rev. A **25**, 2473 (1982).
 [11] C.A. Lutken and F. Ravndal, Phys. Rev. A **31**, 2082 (1985).
 [12] P.W. Milonni and P.L. Knight, Opt. Commun. **9**, 119 (1973).
 [13] E.A. Hinds, in *Advances in Atomic, Molecular, and Optical Physics*, 28th ed., edited by D. Bates and B. Bederson, (Academic, New York, 1991), Vol. 28.
 [14] S. Haroche, in *Fundamental Systems in Quantum Optics*, edited by J. Dalibard, J.M. Raimond, and J. Zinn-Justin (Elsevier, Amsterdam, 1991).
 [15] *Cavity Quantum Electrodynamics*, edited by P. Berman, in *Advances in Atomic and Molecular Physics*, Supplement 2 (Academic, San Diego, 1994).
 [16] E.T. Jaynes and F.W. Cummings, Proc. IEEE **51**, 89 (1963).
 [17] M. Tavis and F.W. Cummings, Phys. Rev. **170**, 379 (1968).
 [18] M. Tavis and F.W. Cummings, Phys. Rev. **188**, 692 (1969).
 [19] M. Gross, P. Goy, C. Fabre, S. Haroche, and J.M. Raimond, Phys. Rev. Lett. **43**, 343 (1979).
 [20] M. Brune, J.M. Raimond, P. Goy, L. Davidovich, and S. Haroche, Phys. Rev. Lett. **59**, 1899 (1987).
 [21] D. Meschede, H. Walther, and G. Muller, Phys. Rev. Lett. **54**, 551 (1985).
 [22] G. Rempe, H. Walther, and N. Klein, Phys. Rev. Lett. **58**, 353 (1987).
 [23] G. Rempe, F. Schmidt-Kaler, and H. Walther, Phys. Rev. Lett. **64**, 2783 (1990).
 [24] Y. Kaluzny, P. Goy, M. Gross, J.M. Raimond, and S. Haroche, Phys. Rev. Lett. **51**, 1175 (1983).
 [25] R.J. Brecha, L.A. Orozco, M.G. Raizen, Min Xiao, and H.J. Kimble, J. Opt. Soc. Am. B **3**, 238 (1986).
 [26] M.G. Raizen, R.J. Thompson, R.J. Brecha, H.J. Kimble, and H.J. Carmichael, Phys. Rev. Lett. **63**, 240 (1989).
 [27] Y. Zhu, D.J. Gauthier, S.E. Morin, Q. Wu, H.J. Carmichael, and T.W. Mossberg, Phys. Rev. Lett. **64**, 2499 (1989).
 [28] R. J. Thompson, G. Rempe, and H. J. Kimble, Phys. Rev. Lett. **68**, 1132 (1992).
 [29] R.J. Brecha, L.A. Orozco, M.G. Raizen, Min Xiao, and H.J. Kimble, J. Opt. Soc. Am. B **12**, 2329 (1995).
 [30] G. Rempe, R.J. Thompson, R.J. Brecha, W.D. Lee, and H.J. Kimble, Phys. Rev. Lett. **67**, 1727 (1991).
 [31] B. R. Mollow, Phys. Rev. **188**, 1969 (1969).
 [32] H.J. Carmichael and D.F. Walls, J. Phys. B **9**, L43 (1976).
 [33] R.E. Grove, F.Y. Wu, and S. Ezekiel, Phys. Rev. A **15**, 227 (1977).
 [34] H.J. Kimble, M. Dagenais, and L. Mandel, Phys. Rev. Lett. **39**, 691 (1977); Phys. Rev. A **18**, 201 (1978).
 [35] J.D. Cresser, J. Hager, G. Leuchs, F.-M. Rateike, and H. Walther, *Dissipative Systems in Quantum Optics*, edited by R. Bonafacio and L. Lugiato (Springer-Verlag, Berlin, 1982).
 [36] D.F. Walls and P. Zoller, Phys. Rev. Lett. **47**, 709 (1981).
 [37] H.J. Carmichael, Phys. Rev. A **33**, 3262 (1985).
 [38] C.W. Gardiner, *Handbook of Stochastic Methods in Physics, Chemistry, and Natural Sciences* (Springer-Verlag, Berlin, 1983).
 [39] H.J. Carmichael, *Statistical Methods in Quantum Optics I* (Springer-Verlag, Berlin, 1999).
 [40] J.J. Sanchez-Mondragon, N.B. Narozhny, and J.H. Eberly, Phys. Rev. Lett. **51**, 550 (1983).
 [41] H.J. Carmichael, R.J. Brecha, M.G. Raizen, H.J. Kimble, and P.R. Rice, Phys. Rev. A **40**, 5516 (1989).
 [42] P.R. Rice and H.J. Carmichael, IEEE J. Quantum Electron. **24**, 1351 (1988).
 [43] H.J. Carmichael, R.J. Brecha, and P.R. Rice, Opt. Commun. **82**, 73 (1991).
 [44] G. Rempe, R.J. Thompson, R.J. Brecha, W.D. Lee, and H.J. Kimble, Phys. Rev. Lett. **67**, 1727 (1991).
 [45] S.L. Mielke, G.T. Foster, and L.A. Orozco, Phys. Rev. Lett. **80**, 3948 (1998).
 [46] H.J. Carmichael, S. Singh, R. Vyas, and P.R. Rice, Phys. Rev. A **39**, 1200 (1989).
 [47] H.J. Carmichael, *An Open Systems Approach to Quantum Optics* (Springer-Verlag, Berlin, 1993).
 [48] J. Dalibard, Y. Castin, and K. Molmer, Phys. Rev. Lett. **68**, 580 (1992).
 [49] R. Dum, P. Zoller, and H. Ritsch, Phys. Rev. A **45**, 4879 (1992).
 [50] P. Alsing and C. Savage (unpublished).
 [51] J.P. Clemens and P.R. Rice (unpublished).
 [52] M. Xiao, doctoral dissertation, University of Texas at Austin,

- 1988, R. J. Brecha, doctoral dissertation, University of Texas at Austin, 1992.
- [53] See, for example, L. A. Lugiato, in *Progress in Optics*, edited by E. Wolf (North-Holland, Amsterdam, 1984), Vol. XXI.
- [54] R.J. Glauber, *Phys. Rev.* **131**, 2766 (1963).
- [55] E.C.G. Sudarshan, *Phys. Rev. Lett.* **10**, 277 (1963).
- [56] P.D. Drummond and C.W. Gardiner, *J. Phys. A* **13**, 2353 (1980).
- [57] H.J. Carmichael, in *Frontiers in Quantum Optics*, edited by E.R. Pike (Adam Hilger, Bristol, 1986).
- [58] A.M. Smith and C.W. Gardiner, *Phys. Rev. A* **39**, 3511 (1989).
- [59] P.D. Drummond and I.K. Mortimer, *J. Comput. Phys.* **93**, 144 (1991).
- [60] R. Loudon, *The Quantum Theory of Light* (Oxford University Press, Oxford, 1983).
- [61] H. Mabuchi, Q.A. Turchette, M.S. Chapman, and H.J. Kimble, *Opt. Lett.* **21**, 1393 (1996).
- [62] J. Ng and L.A. Orozco (unpublished).